Exact Potts Model Partition Functions for Strips of the Triangular Lattice

Shu-Chiuan Chang

C. N. Yang Institute for Theoretical Physics
State University of New York
Stony Brook, N. Y. 11794-3840
USA
After 9/10/2002: Department of Applied Physics:
Faculty of Science
Tokyo University of Science
1-3 Kagurazaka, Shinjuku-ku
Tokyo 162-8601
JAPAN
chang@rs.kagu.tus.ac.jp

Jesper Lykke Jacobsen

Laboratoire de Physique Théorique et Modèles Statistiques
Université Paris-Sud
Bâtiment 100
F-91405 Orsay
FRANCE
jacobsen@ipno.in2p3.fr

Jesús Salas

Departamento de Física Teórica
Facultad de Ciencias, Universidad de Zaragoza
Zaragoza 50009
SPAIN
After 1 Oct. 2003: Departmento de Matemáticas
Universidad Carlos III de Madrid
Avda. de la Universidad, 38
28911 Leganés, SPAIN
jsalas@math.uc3m.es

Robert Shrock

C. N. Yang Institute for Theoretical Physics
State University of New York
Stony Brook, N. Y. 11794-3840
USA
robert.shrock@sunysb.edu

November 27, 2002
revised April 29, 2003

Abstract

We present exact calculations of the Potts model partition function $Z(G, q, v)$ for arbitrary q and temperature-like variable v on n-vertex strip graphs G of the triangular lattice for a variety of transverse widths equal to L vertices and for arbitrarily great length equal to m vertices, with free longitudinal boundary conditions and free and periodic transverse boundary conditions. These partition functions have the form $Z(G, q, v) = \sum_{j=1}^{N_{Z,G,\lambda}} c_{Z,G,j} (\lambda_{Z,G,j})^{m-1}$. We give general formulas for $N_{Z,G,j}$ and its specialization to $v = -1$ for arbitrary L. The free energy is calculated exactly for the infinite-length limit of the graphs, and the thermodynamics is discussed. It is shown how the internal energy calculated for the case of cylindrical boundary conditions is connected with critical quantities for the Potts model on the infinite triangular lattice. Considering the full generalization to arbitrary complex q and v, we determine the singular locus $\mathcal{B}$, arising as the accumulation set of partition function zeros as $m \to \infty$, in the q plane for fixed v and in the v plane for fixed q. Explicit results for partition functions are given in the text for $L = 3$ (free) and $L = 3, 4$ (cylindrical), and plots of partition function zeros and their asymptotic accumulation sets are given for L up to 5. A new estimate for the phase transition temperature of the $q = 3$ Potts antiferromagnet on the 2D triangular lattice is given.

1   Introduction

The q-state Potts model has served as a valuable model for the study of phase transitions and critical phenomena [1, 2]. In this paper we present some theorems on structural properties of Potts model partition functions on triangular-lattice strips of arbitrary width equal to L vertices and arbitrarily great length equal to m vertices. We also report exact calculations of Potts model partition functions for a number of triangular-lattice strips of various widths and arbitrarily great lengths. Using these results, we consider the limit of infinite length. For this limit we calculate thermodynamic functions and determine the loci in the complex q and temperature planes where the free energy is non-analytic. These loci arise as the continuous accumulation sets of partition-function zeros. This work is an extension to the triangular lattice of our earlier study for the square lattice [3].

Consider a graph $G = (V, E)$, defined by its vertex set V and edge set E. Denote the number of vertices and edges as $|V| \equiv n$ and $|E|$, respectively. For technical simplicity, we restrict to connected loopless graphs. On this graph G, at temperature T, the Potts model is defined by the partition function

$$Z(G, q, v) = \sum_{\{\sigma_n\}} e^{-\beta \mathcal{H}} \tag{1.1}$$

with the (zero-field) Hamiltonian

$$\mathcal{H} = -J \sum_{\langle ij \rangle} \delta_{\sigma_i \sigma_j} \tag{1.2}$$

where $\sigma_i = 1, \ldots, q$ are the spin variables on each vertex $i \in V$; $\beta = (k_B T)^{-1}$; and $\langle ij \rangle \in E$ denotes pairs of adjacent vertices. We use the notation

$$K = \beta J , \quad a = e^K , \quad v = a - 1 \tag{1.3}$$

so that the physical ranges are (i) $a \geq 1$, i.e., $v \geq 0$ corresponding to $\infty \geq T \geq 0$ for the Potts ferromagnet, and (ii) $0 \leq a \leq 1$, i.e., $-1 \leq v \leq 0$, corresponding to $0 \leq T \leq \infty$ for the Potts antiferromagnet. One defines the (reduced) free energy per site $f = -\beta F$, where F is the actual free energy, via

$$f(\{G\}, q, v) = \lim_{n \to \infty} \ln[Z(G, q, v)^{1/n}] \tag{1.4}$$

where we use the symbol $\{G\}$ to denote $\lim_{n \to \infty} G$ for a given family of graphs G.

For our results in this paper we shall consider two types of boundary conditions: free and cylindrical. Here, free boundary conditions mean free in both the transverse and longitudinal directions (the latter being the one that is varied for a fixed width), while cylindrical boundary conditions mean periodic in the transverse direction and free in the longitudinal direction. Exact partition functions for arbitrary q and v have previously been presented for strips of the triangular lattice for width $L = 2$ in [4] and results have been given for $L = 3, 4$ in [5]. Here we shall give new explicit results

using the transfer matrix method (in the Fortuin–Kasteleyn representation [6, 7]) for strips with free and cylindrical boundary conditions with width $L = 3$ (free) in section 3.2 and $L = 3, 4$ (cylindrical) in sections 4.2 and 4.3. We have obtained new algebraic computer results for $4 \leq L \leq 6$ (free) and $5 \leq L \leq 9$ (cylindrical); these are too lengthy to include here but are included in the MATHEMATICA computer file `transfer_Tutte_tri.m` which is available with the electronic version of this paper in the `cond-mat` archive at `http://arXiv.org`. We shall also present plots of partition function zeros and their asymptotic accumulation sets in the limit of infinite length, for widths $2 \leq L \leq 5$. Where our results overlap with those for $L = 2, 3, 4$ given before in [4, 5], they are in agreement. As noted, we shall also give exact results valid for these strips with arbitrary width and length, namely the structural theorems of section 2.

There are several motivations for this work. Clearly, new exact calculations of Potts model partition functions are of value in their own right. In addition, these calculations can give insight into the complex-temperature phase diagram of the two-dimensional (2D) Potts model on a particular lattice. This is useful, since the 2D Potts model has never been solved except in the $q = 2$ Ising case. From a mathematical point of view, the partition function of the Potts model on a graph G is equivalent to the Tutte polynomial on the same graph G (see below). Thus, we can extract very useful combinatorial information on the graph G.

Let $G' = (V, E')$ be a spanning subgraph of G, i.e. a subgraph having the same vertex set V and an edge set $E' \subseteq E$. Then $Z(G, q, v)$ can be written as the sum [8, 6, 7]

$$Z(G, q, v) = \sum_{G' \subseteq G} q^{k(G')} v^{|E'|} \tag{1.5}$$

where $k(G')$ denotes the number of connected components of G'. The formula (1.5) enables one to generalize q from $\mathbb{Z}_+$ to $\mathbb{R}_+$ (keeping v in its physical range), and it also shows that $Z(G, q, v)$ is a polynomial in q and v (equivalently, a).

The Potts model partition function on a graph G is essentially equivalent to the Tutte polynomial [9, 10, 11] and Whitney rank polynomial [12, 2, 13, 14, 15, 16]. Here the Tutte polynomial of an arbitrary graph $G = (V, E)$ is

$$T(G, x, y) = \sum_{G' \subseteq G} (x - 1)^{k(G') - k(G)} (y - 1)^{c(G')} \tag{1.6}$$

where G' again denotes a spanning subgraph of G and $c(G')$ denotes the number of independent circuits in G', satisfying $c(G') = |E'| + k(G') - |V|$. Since we only consider connected graphs G, we have $k(G) = 1$. From (1.5) and (1.6), it follows that the Potts model partition function $Z(G, q, v)$ is related to the Tutte polynomial $T(G, x, y)$ according to

$$Z(G, q, v) = (x - 1)^{k(G)} (y - 1)^{|V|} T(G, x, y) \tag{1.7}$$

where

$$x = 1 + \frac{q}{v} \tag{1.8a}$$

$$y = a = v + 1 \tag{1.8b}$$

4

so that

$$q = (x - 1)(y - 1) \tag{1.9}$$

In addition to the works [4, 5], previous exact calculations of Potts model partition functions for arbitrary q and v on lattice strips and/or studies of their properties include [3, 17, 18, 19, 20, 22, 23, 24, 25, 26]; a related early study of chromatic and Tutte polynomials for recursive families of graphs is [27].

Various special cases of the Potts model partition function are of interest. One special case is the zero-temperature limit of the Potts antiferromagnet, i.e., $v = -1$. For sufficiently large q, on a given lattice or graph G, this exhibits nonzero ground state entropy S_0 (without frustration). This is equivalent to a ground state degeneracy per site (vertex), $W > 1$, since $S_0 = k_B \ln W$. The $T = 0$ partition function of the q-state Potts antiferromagnet on G satisfies

$$Z(G, q, -1) = P(G, q) \tag{1.10}$$

where $P(G, q)$ is the chromatic polynomial (in q) expressing the number of ways of coloring the vertices of the graph G with q colors such that no two adjacent vertices have the same color [8, 14, 28, 29]. The minimum number of colors necessary for this coloring is the chromatic number of G, denoted $\chi(G)$. We have

$$W(\{G\}, q) = \lim_{n \to \infty} P(G, q)^{1/n} \tag{1.11}$$

In the context of our current work we recall that the chromatic number for the 2D triangular lattice is $\chi(\mathrm{tri}) = 3$. This chromatic number also applies to strips of the triangular lattice with free longitudinal boundary conditions and free transverse boundary conditions. For the triangular-lattice strips with cylindrical (i.e., free longitudinal and periodic transverse) boundary conditions, $\chi = 3$ if the width $L = 0$ mod 3 and $\chi = 4$ if $L = 1$ or 2 mod 3. References to papers on the special case $v = -1$ are given, e.g., in [18, 25, 30, 3].

Using the formula (1.5) for $Z(G, q, v)$, one can generalize q from $\mathbb{Z}_+$ not just to $\mathbb{R}_+$ but to $\mathbb{C}$ and v from its physical ferromagnetic and antiferromagnetic ranges $0 \le v \le \infty$ and $-1 \le v \le 0$ to $v \in \mathbb{C}$. A subset of the zeros of Z in the two-complex dimensional space $\mathbb{C}^2$ defined by the pair of variables (q, v) can form an accumulation set in the $n \to \infty$ limit, denoted $\mathcal{B}$, which is the continuous locus of points where the free energy is nonanalytic. This locus is determined as the solution to a certain $\{G\}$-dependent equation. For a given value of v, one can consider this locus in the q plane, and we denote it as $\mathcal{B}_q(\{G\}, v)$. In the special case $v = -1$ where the partition function is equal to the chromatic polynomial, the zeros in q are the chromatic zeros, and $\mathcal{B}_q(\{G\}, v = -1)$ is their continuous accumulation set in the $n \to \infty$ limit. With the exact Potts partition function for arbitrary temperature, one can study $\mathcal{B}_q$ for $v \ne -1$ and, for a given value of q, one can study the continuous accumulation set of the zeros of $Z(G, q, v)$ in the v plane (complex-temperature or Fisher zeros [31] - other early references include [32, 33, 34]). This set will be denoted $\mathcal{B}_v(\{G\}, q)$.

2 General Results for Recursive Families of Graphs

A recursive family of graphs is one in which one constructs successive members of the family in a recursive manner starting from an initial member. Recursive families of graphs that are of particular interest here are strips of regular lattices of a given width L vertices (with free or cylindrical boundary conditions) and arbitrarily great length m vertices (with free boundary conditions).

A general form for the Potts model partition function for the strip graphs considered here is [18]

$$Z(G, q, v) = \sum_{j=1}^{N_{Z,G,\lambda}} c_{G,j} (\lambda_{G,j})^{m-1} \tag{2.1}$$

where the coefficients $c_{G,j}$ and corresponding terms $\lambda_{G,j}$, as well as the total number $N_{Z,G,\lambda}$ of these terms, depend on the type of recursive graph G (width and boundary conditions) but not on its length. (In [18], a slightly different labelling convention was used so that $\lambda_{G,j}^m$ rather than $\lambda_{G,j}^{m-1}$ appeared in the summand of eq. (2.1).) In the special case $v = -1$ where Z reduces to the chromatic polynomial (zero-temperature Potts antiferromagnet), eq. (2.1) reduces to the form [35]

$$P(G, q) = \sum_{j=1}^{N_{P,G,\lambda}} c_{G,j} (\lambda_{P,G,j})^{m-1} \tag{2.2}$$

For the lattice strips of interest here, we define the following explicit notation. Let $N_{Z,\text{sq},\text{BC}_t \text{ BC}_\ell,L,\lambda}$ denote the total number of λ's for the square-lattice strip with the transverse (t) and longitudinal (ℓ) boundary conditions BC_t and BC_ℓ of width L. Henceforth where no confusion will result, we shall suppress the λ subscript. The explicit labels are $N_{Z,\text{sq},\text{FF},L}$ and $N_{Z,\text{tri},\text{FF},L}$ for the strips of the square and triangular lattices with free boundary conditions, and $N_{Z,\text{sq},\text{PF},L}$ and $N_{Z,\text{tri},\text{PF},L}$ for the strips of these respective lattices with cylindrical boundary conditions.

For the lattice strip graphs of interest here we can express the partition function via a transfer matrix T (in the Fortuin-Kasteleyn representation) of fixed size $M \times M$:

$$Z(G, q, v) = \text{tr} \left[A(q, v) \cdot \mathsf{T}(q, v)^{m-1} \right] \tag{2.3}$$

which then yields the form (2.1). Since the transfer matrix T and the boundary-condition matrix A are polynomials in q and v, it follows that the eigenvalues $\{\lambda_k\}$ of the transfer matrix and the coefficients $c_{G,j}$ are algebraic functions of q and v.

One of the basic structural properties of the Potts model partition function on a given strip is the number of different eigenvalues of the transfer matrix (in the Fortuin-Kasteleyn representation), $N_{Z,G,\text{BC},L}$, in eq. (2.1). In [3], in addition to proving various formulas for these numbers for certain strip graphs, we presented a conjecture (denoted Conjecture 3 in [3] and given as Theorem 4.3.5 by one of us (S.-C.C.) in [36]). We now give the proof of this result.

Theorem 2.1 *For arbitrary L,*

$$2N_{Z,\text{sq,PF},L} - N_{Z,\text{tri,PF},L} = \begin{cases} N_{Z,\text{sqtri,FP},\frac{L}{2}} & \text{for even } L \\ \frac{1}{2}N_{Z,\text{sqtri,FP},\frac{L+1}{2}} & \text{for odd } L \end{cases} \tag{2.4}$$

where the quantity $N_{Z,\text{sqtri,FP},L}$ is given by [20]:

$$N_{Z,\text{sqtri,FP},L} = \binom{2L}{L} \tag{2.5}$$

Proof We recall first that the quantity $2N_{Z,\text{sq,FF},L} - N_{Z,\text{tri,FF},L}$ discussed in [3] gives the number of non-crossing partitions for a transverse slice of these two respective strips (which is the path graph T_L) such that these partitions are symmetric under reflection about the longitudinal axis. The quantity $2N_{Z,\text{sq,PF},L} - N_{Z,\text{tri,PF},L}$ gives the corresponding number of non-crossing partitions for a transverse slice (which is the circuit graph C_L) of the two respective cylindrical strips such that these partitions are symmetric under reflections about the longitudinal axis and rotations around this axis (the latter being included since there is no special azimuthal direction). We shall prove eq. (2.4) for odd L first and then for even L.

For odd L, let $n = (L+1)/2$, and denote $2N_{Z,\text{sq,PF},L=2n-1} - N_{Z,\text{tri,PF},L=2n-1}$ as X_n for simplicity. Consider a transverse slice with periodic boundary conditions. Since this is topologically invariant under rotations around the longitudinal axis, we can label one vertex as 1 and other vertices $2, 3, \ldots, n, n', (n-1)', \ldots, 2'$, in a counterclockwise manner (relative to a specified longitudinal direction), and consider the reflection symmetry with respect to the longitudinal axis passing through vertex 1. In order to classify the types of colorings of the vertices, we shall introduce diagrams consisting of the L vertices on this transverse slice. In this context, we shall refer to two vertices as being "connected" if these have the same color and shall denote this by using the Kronecker delta function.

The sets $\mathbf{P}_{X_n}$ of partitions for $n = 1, 2, 3$ that are invariant under this reflection symmetry are: $\mathbf{P}_{X_1} = \{1\}$, $\mathbf{P}_{X_2} = \{1, \delta_{2,2'}, \delta_{1,2}\delta_{1,2'} = \delta_{1,2,2'}\}$, and

$$\begin{aligned} \mathbf{P}_{X_3} = \{ &1, \delta_{2,2'}, \delta_{3,3'}, \delta_{1,2,2'}, \delta_{1,3,3'}, \delta_{2,3}\delta_{2',3'}, \delta_{2,2'}\delta_{3,3'}, \\ &\delta_{2,3,2',3'}, \delta_{1,2,2'}\delta_{3,3'}, \delta_{1,2,3,2',3'} \} \end{aligned} \tag{2.6}$$

We can classify these partitions into cases that have m vertices on one side of the slice (including vertex 1) connected to at least one other vertex (on the same side or the other side, indicated by the primes above), where $0 \leq m \leq n$. For $m = 0$, this is the partition 1, that is the identity partition, defined as the one in which all blocks are "singletons", i.e., there are no connections in the sense given above. For $m = 1$, there is only one possibility: $\delta_{x_1,x_1'}$, where $2 \leq x_1 \leq n$. For $m = 2$, let us denote the connected vertices as x_1, x_2 and, with no loss of generality, take $x_1 < x_2$; then there are the partitions δ_{x_1,x_2}, $\delta_{x_1,x_2,x_1'}$, and $\delta_{x_1,x_1'}\delta_{x_2,x_2'}$. For the first case, x_1 can be vertex 1, but for the second and third cases, $2 \leq x_1 \leq n$ since x_1 and x_1' are different vertices. The corresponding partitions $\delta_{x_1',x_2'}$ for the first and second cases can be obtained by reflection symmetry from the ones that we have

listed and hence, for simplicity, are not shown. With no loss of generality, we take $x_1 < x_2 < \ldots < x_m$. For $m = 3$, the partitions are $\delta_{x_1,x_2}\delta_{x_3,x'_3}$, δ_{x_1,x_2,x_3}, $\delta_{x_1,x_2,x'_1}\delta_{x_3,x'_3}$, $\delta_{x_1,x_2,x_3,x'_1}$, $\delta_{x_1,x'_1}\delta_{x_2,x_3}$, $\delta_{x_1,x'_1}\delta_{x_2,x_3,x'_2}$, $\delta_{x_1,x'_1}\delta_{x_2,x'_2}\delta_{x_3,x'_3}$. Having given these illustrations of the specific partitions for $0 \leq m \leq 3$, we next proceed to the general case.

The partitions that have m vertices on one side of the slice connected to as least one other vertex (on the same or opposite side) can be classified further. Let us denote a_m as the number of cases where the vertex x_1 has only the connection δ_{x_1,x'_1} for $1 \leq m$. In these cases, x_1 cannot be vertex 1, and the number of the partitions for each $m \leq n - 1$ is $\binom{n-1}{m}$. The last three partitions of $m = 3$ given above are examples of these cases. We denote b_m as the number of cases where the vertex x_1 has connection to at least one unprimed vertex with or without δ_{x_1,x'_1} for $2 \leq m$. The first and second partitions for $m = 3$ are examples of these cases without δ_{x_1,x'_1}, and the third and fourth partitions for $m = 3$ are examples of these cases with δ_{x_1,x'_1}. Notice that while x_1 cannot be vertex 1 for the cases with δ_{x_1,x'_1}, which have the number of partitions $\binom{n-1}{m}$ for each $m \leq n - 1$, x_1 can be vertex 1 for the cases without δ_{x_1,x'_1}, and the number of partitions for each $m \leq n$ is $\binom{n}{m}$. Therefore,

$$X_n = 1 + \sum_{m=1}^{n-1} a_m \binom{n-1}{m} + \sum_{m=2}^{n-1} b_m \binom{n-1}{m} + \sum_{m=2}^{n} b_m \binom{n}{m} \tag{2.7}$$

Next, we shall obtain expressions for a_m and b_m. The cases for a_m can be obtained from all the cases with $m - 1$ vertices by changing x_i to x_{i+1} for $1 \leq i \leq m - 1$ and adding δ_{x_1,x'_1}, i.e., a_m is the same as the total number of the cases with $m - 1$ vertices,

$$a_m = a_{m-1} + 2b_{m-1} \tag{2.8}$$

Now consider the cases for b_m without δ_{x_1,x'_1}. These can be further divided into two possibilities: the cases with δ_{x_1,x_2} and the cases with δ_{x_1,x_i} where $2 < i \leq m$. Denote the numbers of these two possibilities as d_m and e_m, respectively. Clearly,

$$b_m = d_m + e_m \tag{2.9}$$

The cases for d_m can be obtained from the cases for b_{m-1} by changing x_i to x_{i+1} for $1 \leq i \leq m - 1$ and adding δ_{x_1,x_2}, and from all the cases with $m - 2$ vertices, where the number is a_{m-1}, by changing x_i to x_{i+2} for $1 \leq i \leq m - 2$ and adding δ_{x_1,x_2}. Therefore,

$$d_m = a_{m-1} + b_{m-1} \tag{2.10}$$

The cases for e_m can be obtained from the cases for d_{m-2} by changing x_i to x_{i+2} for $2 \leq i \leq m - 2$ and adding δ_{x_2,x_3}, from the cases for d_{m-3} by changing x_i to x_{i+3} for $2 \leq i \leq m - 3$ and adding δ_{x_2,x_3,x_4}, etc. In general, the cases for e_m are obtained from the cases for $d_{m-\ell}$ by changing x_i to $x_{i+\ell}$ for $2 \leq i \leq m - \ell$ and $2 \leq \ell \leq m - 2$, and adding a set of ℓ vertices, where all the vertices in this set must have at least one connection to at least one other vertex in this set without reflection or rotation symmetry. The number of all possible connections of this set with ℓ vertices is the

Riordan number (given as sequence A005043 in [37]), which will be denoted as r_ℓ and may be defined via the generating function [38]

$$R(z) = \frac{1 + z - (1 - 2z - 3z^2)^{1/2}}{2z(1+z)} = \sum_{\ell=0}^{\infty} r_\ell z^\ell \qquad (2.11)$$

Therefore,

$$e_m = \sum_{\ell=2}^{m-2} d_{m-\ell}\, r_\ell \qquad (2.12)$$

In terms of generating functions

$$
\begin{aligned}
A(z) &= a_1 z + a_2 z^2 + a_3 z^3 + \ldots \\[2mm]
B(z) &= b_2 z^2 + b_3 z^3 + b_4 z^4 + \ldots \\[2mm]
D(z) &= d_2 z^2 + d_3 z^3 + d_4 z^4 + \ldots \\[2mm]
E(z) &= e_4 z^4 + e_5 z^5 + e_6 z^6 + \ldots \\[2mm]
R(z) &= 1 + r_2 z^2 + r_3 z^3 + r_4 z^4 + \ldots
\end{aligned}
\qquad (2.13)
$$

we can re-express eqs. (2.8) to (2.12) as

$$
\begin{aligned}
\frac{A(z) - a_1 z}{z} &= A(z) + 2B(z) \\[2mm]
B(z) &= D(z) + E(z) \\[2mm]
\frac{D(z)}{z} &= A(z) + B(z) \\[2mm]
E(z) &= D(z)(R(z) - 1)
\end{aligned}
\qquad (2.14)
$$

We find

$$A(z) = \frac{z}{\sqrt{1 - 2z - 3z^2}} \qquad (2.15)$$

The coefficients in the expansion of $A(z)$ in eq. (2.13) are, up to a shift, the central trinomial coefficients (given as sequence A002426 in [37]), i.e., for each value $1 \le m$ the largest coefficient of $(1 + z + z^2)^{m-1}$. Next,

$$B(z) = \frac{1}{2}\left[\frac{1 - z}{\sqrt{1 - 2z - 3z^2}} - 1\right] \qquad (2.16)$$

The coefficients in the expansion of $B(z)$ in (2.13) are given by the coefficients for the next-to-central column in the expansion of $(1 + z + z^2)^{m-1}$ for $1 \le m$ (listed as sequence A005717 in [37]). For $D(z)$ we have the closed form

$$D(z) = \frac{z}{2}\left[\sqrt{\frac{1 + z}{1 - 3z}} - 1\right] \qquad (2.17)$$

9

The coefficients in the expansion of $D(z)$ in (2.13) are the numbers of directed animals of size $m - 1$ on the square lattice for $1 \leq m$ (given as sequence A005773 in [37]). Finally, we have

$$E(z) = z \frac{1 - 3z + (1 - 2z)\sqrt{1 - 2z - 3z^2}}{1 - 2z - 3z^2 + (3z - 1)\sqrt{1 - 2z - 3z^2}} - 1 + z \qquad (2.18)$$

The coefficients in the expansion of $E(z)$ in (2.13) are the coefficients forming the second column from the center, in a tabular format, in the expansion of $(1+z+z^2)^{m-2}$ for $2 \leq m$ (given as sequence A014531 in [37]).

Recall the binomial transformation for two sequences of numbers $[s_0, s_1, s_2, \ldots]$, $[t_0, t_1, t_2, \ldots]$ with generating functions $S(z) = \sum_{n=0}^{\infty} s_n z^n$ and $T(z) = \sum_{n=0}^{\infty} t_n z^n$. If these sequences have the relation

$$t_n = \sum_{m=0}^{n} \binom{n}{m} s_m , \qquad (2.19)$$

then [39]

$$T(z) = \frac{1}{1 - z} S\left(\frac{z}{1 - z}\right) \qquad (2.20)$$

In our case, if the generating function of X_n is $X(z) = \sum_{n=1}^{\infty} X_n z^n$, then we can combine eqs. (2.7), (2.15) and (2.16) to get

$$\begin{aligned}
X(z) &= \frac{1}{1 - z} - 1 + \frac{z}{1 - z} A\left(\frac{z}{1 - z}\right) + \frac{z}{1 - z} B\left(\frac{z}{1 - z}\right) + \frac{1}{1 - z} B\left(\frac{z}{1 - z}\right) \\
&= \frac{1}{2}\left[\frac{1}{\sqrt{1 - 4z}} - 1\right] \qquad (2.21)
\end{aligned}$$

This has the expansion

$$X(z) = \sum_{n=1}^{\infty} \binom{2n - 1}{n} z^n \qquad (2.22)$$

Note that $\binom{2n-1}{n} = \frac{1}{2}\binom{2n}{n} = \frac{1}{2}\binom{L+1}{(L+1)/2}$ (given as sequence A001700 in [37]).

Let us next proceed to consider the number of non-crossing partitions for a slice of the transverse vertices which has periodic boundary conditions and reflection symmetry for even L. Denote $n = L/2$, and $2N_{Z,\text{sq,PF},L=2n} - N_{Z,\text{tri,PF},L=2n}$ by Y_n for simplicity. There are two possibilities: the reflection axis does not go through any vertex or goes through two vertices. These possibilities will be denoted as type I and and type II partitions, respectively, and the number of partitions of each of these two types as Y_n^{I} and Y_n^{II}. For type I partitions, label the vertices on one side of the reflection axis as 1, 2,..., n and the corresponding reflected vertices as $1', 2', \ldots, n'$ on the other side. For type II partitions, label the vertices as 1, 2, ..., n, $n + 1$, n', ..., $2'$, where vertices 1 and $n + 1$ are on the reflection axis. The sets $\mathbf{P}_{Y_n^{\text{I}}}$ of type I partitions for $n = 1, 2$ having this reflection symmetry are: $\mathbf{P}_{Y_1^{\text{I}}} = \{1, \delta_{1,1'}\}$ and $\mathbf{P}_{Y_2^{\text{I}}} = \{1, \delta_{1,1'}, \delta_{2,2'}, \delta_{1,2}\delta_{1',2'}, \delta_{1,2,1'}, \delta_{1,1'}\delta_{2,2'}\}$. The sets $\mathbf{P}_{Y_n^{\text{II}}}$ of type II partitions for $n = 1, 2$ having this reflection symmetry are: $\mathbf{P}_{Y_1^{\text{II}}} = \{1, \delta_{1,2}\}$

and $\mathbf{P}_{Y_2^{\mathrm{II}}} = \{1, \delta_{2,2'}, \delta_{1,3}, \delta_{1,2,2'}, \delta_{2,3,2'}, \delta_{1,2,3,2',3'}\}$. We notice that partitions 1, i.e. identity and $\delta_{1,2,\ldots,L}$ (i.e., a unique block) are both contained in the type I and type II classes of partitions. Since we have rotational symmetry, the partitions which are not symmetric with respect to the central axis perpendicular to the reflection axis are counted twice in either type I or type II classes of partitions. A similar statement applies to the partitions which are symmetric with respect to the axis perpendicular to the reflection axis if L is a multiple of 4. If L is not a multiple of 4, the partitions that are symmetric with respect to the perpendicular axis are counted once in both type I and type II classes. Therefore, $2Y_n$ is the sum of all possible partitions in these two classes of partitions.

We again classify these partitions into cases which have m vertices on one side of the slice connected to at least one other vertex (including vertex 1 and vertex $n+1$ for type II partitions). It is clear that $0 \leq m \leq n$ for type I partitions and $0 \leq m \leq n+1$ for type II partitions. Let us consider type I first. For $m = 0$, there is the partition 1 (identity). For $m = 1$, there is only one possibility: $\delta_{x_1,x_1'}$, where $1 \leq x_1 \leq n$. For $m = 2$, there are δ_{x_1,x_2}, $\delta_{x_1,x_2,x_1'}$ and $\delta_{x_1,x_1'}\delta_{x_2,x_2'}$, where $x_1 < x_2$. The corresponding $\delta_{x_1',x_2'}$ for the first and second cases are not shown for simplicity. We shall again take $x_1 < x_2 < \ldots < x_m$. The number of the cases with m vertices connected is $a_m + 2b_m = a_{m+1}$ as discussed above eq. (2.8), and the number of the partitions is $\binom{n}{m}$ for each $0 \leq m \leq n$. Therefore,

$$Y_n^{\mathrm{I}} = \sum_{m=0}^{n} a_{m+1} \binom{n}{m} \quad \text{for } 1 \leq n \tag{2.23}$$

Let the generating function of Y_n^{I} be $Y^{\mathrm{I}}(z) = \sum_{n=1}^{\infty} Y_n^{\mathrm{I}} z^n$. Using eq. (2.15) and modifying eq. (2.20), we have

$$Y^{\mathrm{I}}(z) = \frac{1}{1-z} \left[\frac{A\left(\frac{z}{1-z}\right)}{\frac{z}{1-z}} \right] - a_1 = \frac{1}{\sqrt{1-4z}} - 1 \tag{2.24}$$

For type II partitions, neither vertex 1 nor vertex $n+1$ has a corresponding symmetric partner, $1'$ and $(n+1)'$, respectively. We have to classify the cases where x_1 is only connected to at least one other unprimed vertex (in these cases, x_1 can be vertex 1), the number of which cases was denoted b_m earlier, into two possibilities: the cases where x_m is only connected to at least one other unprimed vertex (so that x_m can be vertex $n+1$), and the cases where x_m is connected to x_m' (so that x_m cannot be vertex $n+1$) among other possible connections. The number of partitions for these two possibilities will be denoted as f_m for $2 \leq m$ and h_m for $3 \leq m$, respectively. The partitions where x_1 is connected to x_1', i.e., $\delta_{x_1,x_1'}$, among other possible connections can also be classified into two possibilities: the cases where x_m is only connected to other unprimed vertices, and the cases where x_m is connected to x_m' among other possible connections. The number of partitions for these two possibilities will be denoted as h_m' for $3 \leq m$ and i_m for $1 \leq m$, respectively. Notice that $h_m' = h_m$ because of the reflection symmetry. We shall need another set of partitions where x_1 is connected to x_m with possible connection to other unprimed vertices, and all the

other vertices are connected to at least one other unprimed vertex; we denote the number of partitions for them as j_m for $2 \leq m$. If we add an additional connection $\delta_{x_1, x_1'}$ to these partitions, and denote the number of partitions as k_m, then $k_1 = 1$ and $k_m = j_m$ for $2 \leq m$.

For the cases for f_m, x_1 and x_m can be vertices 1 and $n+1$, respectively, so the number of the partitions is $\binom{n+1}{m}$ for each m. For the cases for h_m, x_1 can be vertex 1 but x_m cannot be vertex $n+1$, so the number of the partitions is $\binom{n}{m}$ for each m. For the cases for i_m, neither x_1 can be vertex 1 nor x_m can be vertex $n+1$, so the number of the partitions is $\binom{n-1}{m}$ for each m. Therefore,

$$Y_n^{\mathrm{II}} = 1 + \sum_{m=2}^{n+1} f_m \binom{n+1}{m} + 2 \sum_{m=3}^{n} h_m \binom{n}{m} + \sum_{m=1}^{n-1} i_m \binom{n-1}{m} \tag{2.25}$$

We next obtain expressions for f_m, h_m and i_m. From the definitions,

$$f_m + h_m = b_m \tag{2.26}$$

and

$$h_m' + i_m = a_m + b_m = d_{m+1} \ , \tag{2.27}$$

where we use eq. (2.10). The cases for f_m include all the cases for j_m, plus the cases for both f_{m-2} and h_{m-2} with the additional connection δ_{x_{m-1}, x_m}, plus the cases for both f_{m-3} and h_{m-3} with the additional connection $\delta_{x_{m-2}, x_{m-1}, x_m}$, etc. We have

$$f_m = j_m + \sum_{\ell=2}^{m-2} j_\ell \, [f_{m-\ell} + h_{m-\ell}] = j_m + \sum_{\ell=2}^{m-2} j_\ell \, b_{m-\ell} \tag{2.28}$$

The cases for h_m can be obtained by adding $\delta_{x_m, x_m'}$ to the cases for f_{m-1} and h_{m-1}, and adding $\delta_{x_{m-1}, x_m, x_m'}$ to the cases for f_{m-2} and h_{m-2}, etc. We have

$$h_m = \sum_{\ell=1}^{m-2} k_\ell \, [f_{m-\ell} + h_{m-\ell}] = \sum_{\ell=1}^{m-2} k_\ell \, b_{m-\ell} \tag{2.29}$$

The cases for h_m' can be obtained by adding δ_{x_{m-1}, x_m} to the cases for h_{m-2}' and i_{m-2}, and adding $\delta_{x_{m-2}, x_{m-1}, x_m}$ to the cases for h_{m-3}' and i_{m-3}, etc. We have

$$h_m' = \sum_{\ell=2}^{m-1} j_\ell \, [h_{m-\ell}' + i_{m-\ell}] = \sum_{\ell=2}^{m-1} j_\ell \, d_{m-\ell+1} \ , \tag{2.30}$$

which should be equal to h_m, as mentioned before. The cases for i_m include all the cases for k_m, plus the cases for both h_{m-1}' and i_{m-1} with additional connection $\delta_{x_m, x_m'}$, plus the cases for both h_{m-2}' and i_{m-2} with additional connection $\delta_{x_{m-1}, x_m, x_m'}$, etc. We have

$$i_m = k_m + \sum_{\ell=1}^{m-1} k_\ell \, [h_{m-\ell}' + i_{m-\ell}] = k_m + \sum_{\ell=1}^{m-1} k_\ell \, d_{m-\ell+1} \tag{2.31}$$

12

The cases for j_m can be obtained from the cases for r_m by removing the cases for r_{m-2} with additional δ_{x_{m-1},x_m}, removing the cases for r_{m-3} with additional $\delta_{x_{m-2},x_{m-1},x_m}$, etc. We have

$$j_m = r_m - \sum_{\ell=2}^{m-2} j_\ell\, r_{m-\ell} \tag{2.32}$$

In terms of the generating functions

$$
\begin{aligned}
F(z) &= f_2 z^2 + f_3 z^3 + f_4 z^4 + \ldots \\[4pt]
H(z) &= H(z)' = h_3 z^3 + h_4 z^4 + h_5 z^5 + \ldots \\[4pt]
I(z) &= i_1 z + i_2 z^2 + i_3 z^3 + \ldots \\[4pt]
J(z) &= j_2 z^2 + j_3 z^3 + j_4 z^4 + \ldots \\[4pt]
K(z) &= k_1 z + k_2 z^2 + k_3 z^3 + \ldots
\end{aligned} \tag{2.33}
$$

we can reexpress eqs. (2.26) to (2.32) as

$$
\begin{aligned}
F(z) + H(z) &= B(z) \\[6pt]
H(z) + I(z) &= \frac{D(z)}{z} \\[6pt]
F(z) &= J(z) + B(z)J(z) \\[6pt]
H(z) &= B(z)K(z) = \frac{D(z)}{z}J(z) \\[6pt]
I(z) &= K(z) + \frac{D(z)}{z}K(z) \\[6pt]
J(z) &= R(z) - 1 - (R(z)-1)J(z) = (R(z)-1)(1-J(z)) \quad (2.34)
\end{aligned}
$$

We find

$$J(z) = \frac{R(z)-1}{R(z)} = \frac{1}{2}(1 - z - \sqrt{1 - 2z - 3z^2})\,, \tag{2.35}$$

which is essentially the Motzkin number [40, 41] (given as sequence A001006 in [37]). This can be understood since the cases for j_m are in one-to-one correspondence with the non-crossing, non-nearest-neighbor partitions of $m-1$ vertices with free boundary condition, as given in eq. (2.1.1) of [3], i.e., $j_m = M_{m-2}$. We also have

$$K(z) = z + J(z) = \frac{1}{2}(1 + z - \sqrt{1 - 2z - 3z^2}) \tag{2.36}$$

The first five equations in eq. (2.34) are redundant, and can be solved to have

$$F(z) = \frac{z^2}{\sqrt{1 - 2z - 3z^2}} = zA(z)\,, \tag{2.37}$$

13

i.e., $f_m = a_{m-1}$, which is the largest coefficient of $(1 + z + z^2)^{m-2}$ for $2 \leq m$. Next, we have

$$H(z) = \frac{1}{2}\left[\left(\frac{1 - 2z}{1 - 3z}\right)\sqrt{1 - 2z - 3z^2} - 1\right] \tag{2.38}$$

The coefficients in the expansion of $H(z)$ are the numbers of directed animals of size $m - 2$ on the square lattice with the first two quadrants (which can grow in right, left and up directions) for $2 \leq m$ (given as sequence A005774 in [37]). Finally,

$$I(z) = z\sqrt{\frac{1 + z}{1 - 3z}} = 2D(z) + z , \tag{2.39}$$

which is given as sequence A0025565 in [37].

Denote the generating function of Y_n^{II} as $Y^{\mathrm{II}}(z) = \sum_{n=1}^{\infty} Y_n^{\mathrm{II}} z^n$. Combining eqs. (2.25), (2.37), (2.38), (2.39), and using the binomial transformation (2.20), we obtain the relation

$$
\begin{aligned}
Y^{\mathrm{II}}(z) &= \frac{1}{1 - z} - 1 + \frac{1}{z(1 - z)}F\left(\frac{z}{1 - z}\right) + \frac{1}{1 - z}H\left(\frac{z}{1 - z}\right) + \frac{z}{1 - z}I\left(\frac{z}{1 - z}\right) \\
&= \frac{1}{1 - z} - 1 + \frac{z}{(1 - z)^2\sqrt{1 - 4z}} + \frac{1}{2(1 - z)^2}\left[\frac{1 - 3z}{\sqrt{1 - 4z}} + z - 1\right] \\
&\quad + \frac{z^2}{(1 - z)^2\sqrt{1 - 4z}} \\
&= \frac{1}{\sqrt{1 - 4z}} - 1 ,
\end{aligned}
\tag{2.40}
$$

which is the same as the $Y^{\mathrm{I}}(z)$ in eq. (2.24). We finally have

$$Y(z) = \frac{Y^{\mathrm{I}}(z) + Y^{\mathrm{II}}(z)}{2} = \frac{1}{\sqrt{1 - 4z}} - 1 , \tag{2.41}$$

which is the generating function of $\binom{2n}{n} = \binom{L}{L/2}$, i.e., the central binomial coefficients given as sequence A000984 in [37].

Eqs. (2.21) and (2.41) prove the theorem for odd and even L, respectively. $\square$

Another structural result was given as Conjecture 4 in [3] and Theorem 4.3.7 in [36] for the number of λ's for the triangular lattice with cylindrical boundary condition for the Potts model partition function. We state this and give the proof.

Theorem 2.2 *For arbitrary L,*

$$N_{Z,\mathrm{tri,PF},L} = \frac{1}{L}\left[C_L + \sum_{d|L;\ 1 \leq d < L} \phi(L/d)\binom{2d}{d}\right] \tag{2.42}$$

where $d|L$ means that d divides L and $\phi(n)$ is the Euler function, equal to the number of positive integers not exceeding the positive integer n and relatively prime to n.

Proof   As shown in [19], $N_{Z,\text{tri,FF},L} = C_L$ is the number of non-crossing partitions of a set of L vertices with free boundary conditions. $LN_{Z,\text{tri,PF},L} - N_{Z,\text{tri,FF},L}$ is equal to $2(L-1)$ for prime L, as shown in [3, 36], since all the partitions of $N_{Z,\text{tri,PF},L}$ have periodicity L for prime L except for the partitions 1 (i.e., all blocks being singletons) and $\delta_{1,2,\ldots,L}$ (i.e., a unique block) which have periodicity 1. Consider a general L and assume that L has the factor d (so that for prime L, d can only be 1 or L). Denote the number of partitions which have periodicity d modulo rotations as $2\alpha_d$. Then

$$LN_{Z,\text{tri,PF},L} - N_{Z,\text{tri,FF},L} = \sum_{d|L} 2\alpha_d(L-d) \tag{2.43}$$

where d are all the positive integers that divide L.

There are two kinds of partitions among $2\alpha_d$, each of which contains α_d specific partitions. The first kind of partitions is defined by the condition that each set of d adjacent vertices does not have connection with any other vertex in the complementary subset of vertices. Let us label the vertices in one set of d vertices as $1,2,\ldots,d$. For $d = 1$, the set of partition is $\{1\}$. For $d = 2$, the set of partition is $\{\delta_{1,2}\}$. For $d = 3$, the set of partitions is $\{\delta_{1,2}, \delta_{1,3}, \delta_{1,2,3}\}$. The second kind of partitions is defined by the condition that all of the first vertices of each of the sets of d vertices are connected to each other. For $d = 1$, the set of partition is $\{\delta_{1,1'}\}$, where $1'$ is the first vertex of the adjacent set of d vertices. For $d = 2$, the set of partition is $\{\delta_{1,1'}\}$. For $d = 3$, the set of partition is $\{\delta_{1,1'}, \delta_{1,1'}\delta_{2,3}, \delta_{1,1',3}\}$. Since there is a one-to-one correspondence between these two kinds of partitions, let us only consider the second kind of the partitions which always have the connection $\delta_{1,1'}$. Denote α'_d as the number of partitions which has periodicity less than or equal to d modulo rotations. This can be written in term of α_d as

$$\alpha'_d = \sum_{d'|d} \alpha_{d'} \tag{2.44}$$

For the set of d vertices, if vertex 1 does not connect to any other vertex except $1'$, the first vertex of an adjacent set, then the number of partitions is equal to $N_{Z,\text{tri,FF},d-1} = C_{d-1}$. If vertex 1 has a connection to vertex b for $1 < b < d$ in addition to vertex $1'$, then the number of partitions is $C_{b-2}C_{d-b}$. The connection of vertex 1 to vertex $d-b+2$ is equivalent to the connection of vertex 1 to vertex b under rotation symmetry, and should not be considered again. Of course, vertex 1 can have connection to more than one vertices in addition to $\delta_{1,1'}$. Therefore, to calculate α'_d, we have to partition d first. For each partition of d, e.g., $[x_1, x_2, \ldots, x_i]$ with $x_1 + x_2 + \ldots + x_i = d$, where i is the numbers of vertices in the set of d vertices connected to vertex 1 (including vertex 1), we multiply all the corresponding C_{x_i-1}'s by the number of different combinations of this partition modulo rotations (thus [2,2,1,1] is the same as [2,1,1,2] and [1,1,2,2], but different from [2,1,2,1]). As an example, for $d = 5$, we have the partitions $5 = 4+1 = 3+2 = 3+1+1 = 2+2+1 = 2+1+1+1 = 1+1+1+1+1$, and therefore

$$\alpha'_5 \;=\; C_4 + \frac{1}{2}C_3C_0\binom{2}{1} + \frac{1}{2}C_2C_1\binom{2}{1} + \frac{1}{3}C_2C_0^2\binom{3}{1} + \frac{1}{3}C_1^2C_0\binom{3}{2}$$

$$+\frac{1}{4}C_1C_0^3\binom{4}{1} + C_0^5\binom{5}{5}$$
$$= 14 + 5 \times 1 + 2 \times 1 + 2 \times 1^2 + 1^2 \times 1 + 1 \times 1^3 + 1^5 = 26 \qquad (2.45)$$

The factors $\frac{1}{2}$, $\frac{1}{3}$, and $\frac{1}{4}$ are included because of the equivalence under rotations.

We find that α'_d is the same as the rooted planar trees with d edges with the property that rotations about the root vertex yield equivalent trees, given as sequence A003239 in [37]. The reason can be explained as follows. Define a "planted" tree as a rooted tree with the property that the root vertex has degree one (where the degree of a vertex is the number of edges connected to it). Now we can construct planted trees from subtrees of the rooted planar tree that are each connected to the root vertex. Note that the number of planted tree with d edges is C_{d-1} [38]. The sequence A003239 also gives the number of necklaces with a total of $2d$ beads where d beads have one color and the other d beads have another color. The explicit formula is

$$\alpha'_d = \frac{1}{2d}\sum_{d'|d}\phi(d/d')\binom{2d'}{d'}, \qquad (2.46)$$

where $\phi(n)$ was defined above after eq. (2.42).

Now the number of partitions that have periodicity equal to d modulo rotations, α_d, is the Möbius transformation [39] of α'_d, given by

$$\alpha_d = \sum_{d'|d}\mu(d/d')\alpha'_{d'} \qquad (2.47)$$

where $\mu(n)$ is the Möbius function, defined as -1 if n is prime, 0 if n has a square factor, and 1 for other n. We find that α_d is listed as sequence A022553 in [37], which is the Lyndon words containing a total of $2d$ letters with d letters of one type, and the other d letters of another. One has the explicit formula

$$\alpha_d = \frac{1}{2d}\sum_{d'|d}\mu(d/d')\binom{2d'}{d'}, \qquad (2.48)$$

i.e., $2d\alpha_d$, is the Möbius transformation of $\binom{2d}{d}$, or equivalently,

$$\binom{2d}{d} = \sum_{d'|d}2d'\alpha_{d'} \qquad (2.49)$$

Therefore, the total number of partitions that have periodicity d modulo rotations is

$$2\alpha_d = \frac{1}{d}\sum_{d'|d}\mu(d/d')\binom{2d'}{d'} \qquad (2.50)$$

This is given as sequence A060165 in [37].

We finally have

$$LN_{Z,\text{tri,PF},L} - N_{Z,\text{tri,FF},L} \;=\; \sum_{d|L} 2\alpha_d(L-d)$$

$$=\; \sum_{d|L} 2L\alpha_d - \binom{2L}{L}$$

$$=\; \sum_{d|L} \frac{L}{d} \sum_{d'|d} \mu(d/d')\binom{2d'}{d'} - \binom{2L}{L}$$

$$=\; \sum_{d'|L} \sum_{d|L; d'|d} \frac{L}{d}\mu(d/d')\binom{2d'}{d'} - \binom{2L}{L}$$

$$=\; \sum_{d'|L} \phi(L/d')\binom{2d'}{d'} - \binom{2L}{L}$$

$$=\; \sum_{d|L;\ 1\le d<L} \phi(L/d)\binom{2d}{d} \tag{2.51}$$

and the theorem follows. $\square$

Theorems 2.1 and 2.2 imply a simple corollary which gives an exact formula for $N_{Z,\text{sq,PF},L}$:

Corollary 2.1 *For arbitrary L,*

$$N_{Z,\text{sq,PF},L} = \frac{1}{2}\left[N_{Z,\text{tri,PF},L} + \binom{L}{[L/2]}\right] \tag{2.52}$$

Proof For even L is trivial. For odd L, we only have to notice that

$$(1/2)\binom{L+1}{(L+1)/2} = \frac{L(L-1)\cdots\frac{L+3}{2}}{(\frac{L-1}{2})!} = \binom{L}{(L-1)/2} = \binom{L}{[L/2]} \tag{2.53}$$

This proves the corollary. $\square$

One of us (S.-C.C.) has presented a conjecture, Conjecture 4.2.2 in [36], which generalizes Theorem 3 in [3] (i.e., Theorem 4.2.6 in [36]). We restate this conjecture here. Consider the number of λ's in the chromatic polynomial for a strip of the triangular lattice with cylindrical boundary conditions:

Conjecture 2.1 *For arbitrary L,*

$$N_{P,\text{tri,PF},L} = \frac{1}{L}\left[d_L + \sum_{d|L;\ 1\le d<L} \phi(L/d)t_d\right] \tag{2.54}$$

where $t_d = a_{d+1}$ is the largest coefficient in the expansion of $(1 + z + z^2)^d$, i.e., the central trinomial coefficient (given as sequence A002426 in [37]), and d_L is essentially the Riordan number r_L (given as sequence A005043 in [37])

$$d_L = \begin{cases} 1 & L = 1 \\ r_L & L \ge 2 \end{cases} \tag{2.55}$$

17

where the reader is cautioned not to confuse the d_L in eq. (2.54) with the different quantity d_m in eqs. (2.9) and (2.10). We can motivate this conjecture as follows. We know that d_L is the number of non-crossing non-nearest-neighbor partitions of a set of L vertices with periodic boundary conditions, as shown in [19]. The number $LN_{P,\text{tri},\text{PF},L} - d_L$ is equal to $L - 1$ for prime L, as shown in [3, 36], since all the partitions of $N_{P,\text{tri},\text{PF},L}$ have periodicity L for prime L except for the partitions 1 (i.e., all blocks being singletons) which have periodicity 1. Consider a general L having the factor d, and denote the number of non-nearest-neighbor partitions that have periodicity d modulo rotations as β_d. Then

$$LN_{P,\text{tri},\text{PF},L} - d_L = \sum_{d|L} \beta_d(L - d) \tag{2.56}$$

There are two kinds of partitions among β_d; we denote the number of these as β_d^{I} and β_d^{II}, respectively. The first kind of partitions is defined by the condition that each set of d adjacent vertices does not have connection to any other vertices in other sets. Label the d vertices as $1,2,\ldots,d$. For $d = 1$, the set of partitions consists of just $\{1\}$. There is no non-nearest-neighbor partition for $d = 2$. For $d = 3$, the set of partitions is $\{\delta_{1,3}\}$. For $d = 4$, the set of partitions is $\{\delta_{1,4}, \delta_{1,3}\}$. The second kind of partitions is defined by the condition that all of the first vertices of each set of d vertices are connected to each other. There is no non-nearest-neighbor partition for $d = 1$. For $d = 2$, the set of partitions is comprised of $\{\delta_{1,1'}\}$, where $1'$ is the first vertex of an adjacent set of d vertices. For $d = 3$, the set of partitions is $\{\delta_{1,1'}\}$. For $d = 4$, the set of partitions is $\{\delta_{1,1'}, \delta_{1,1'}\delta_{2,4}\}$. Notice that for $d = 4$, $\{\delta_{1,1',3}\}$ is the same as $\{\delta_{1,1'}\}$ for $d = 2$, and should not be included to avoid double-counting.

Consider the first kind of partitions. If the first vertex 1 is connected to the last vertex d among other possible connections with other vertices in the set of d vertices, the number of these partitions is r_{d-1}, the Riordan number (given as sequence A005043 in [37]). This can be seen by identifying the vertices 1 and d to form a circuit with $d - 1$ vertices [19]. In addition, the set of d vertices can also be partitioned into several parts where the first and the last vertices of each part are connected, but parts are not connected to each other. To calculate β_d^{I}, we partition d, and apply the same transformation as illustrated in Theorem 2.2 on r_{d-1}, then apply a Möbius transformation. The first few values of β_d^{I} are 1, 0, 1, 2, 5, 11, 28, 68, 174, 445 for $1 \le d \le 10$.

Consider the second kind of partitions. By an argument similar to that given in the proof of Theorem 2.2, if vertex 1 is not connected to any other vertex except $1'$ among the set of d vertices, then the number of partitions is just $N_{P,\text{tri},\text{FF},d-1} = M_{d-2}$. In addition, the vertex 1 can also be connected to other vertices among the set of d vertices. To calculate β_d^{II}, we again partition d, and apply the same transformation, as illustrated in Theorem 2.2 on M_{d-2}. We then apply a Möbius transformation. The first few values of β_d^{II} are 0, 1, 1, 2, 5, 11, 28, 68, 174, 445 for $1 \le d \le 10$. We find that β_d^{I} and β_d^{II} are the same up to $d = 10$, except for $d = 1$ and 2. Although β_d is not listed in [37], we find that the following relation holds up to $d = 10$, and is similar to

eq. (2.50):

$$\beta_d = \frac{1}{d} \sum_{d'|d} \mu(d/d') t_d \tag{2.57}$$

If this is correct for arbitrary d, then the conjecture is proved.

Combining Conjecture 2.1 and Conjecture 1 in [3], we have

Conjecture 2.2 *For arbitrary L,*

$$N_{P,\mathrm{sq},\mathrm{PF},L} = \begin{cases} \frac{1}{2}\left[N_{P,\mathrm{tri},\mathrm{PF},L} + \frac{1}{2}N_{P,\mathrm{sqtri},\mathrm{FP},\frac{L}{2}} \right] & \text{for even } L \\ \frac{1}{2}\left[N_{P,\mathrm{tri},\mathrm{PF},L} + \frac{1}{4}N_{P,\mathrm{sqtri},\mathrm{FP},\frac{L+1}{2}} - \frac{1}{2}r_{\frac{L-1}{2}} \right] & \text{for odd } L \geq 3 \end{cases} \tag{2.58}$$

where $N_{P,\mathrm{sqtri},\mathrm{FP},L}$ was given in [20], and r_n is the Riordan number (given as sequence A005043 in [37]).

3 Potts Model Partition Functions for Triangular-lattice Strips with Free Boundary Conditions

The Potts model partition function $Z(G, q, v)$ for a triangular-lattice strip of width L and length m with free boundary conditions is given by

$$
\begin{align}
Z(L_{\mathrm{F}} \times m_{\mathrm{F}}, q, v) &= \mathbf{v}^{\mathrm{T}} \cdot \mathsf{H} \cdot \mathsf{T}^{m-1} \cdot \mathbf{u}_{\mathrm{id}} \tag{3.1a} \\
&= \mathbf{w}^{\mathrm{T}} \cdot \mathsf{T}^{m-1} \cdot \mathbf{u}_{\mathrm{id}} \tag{3.1b}
\end{align}
$$

where $\mathbf{w}^{\mathrm{T}} = \mathbf{v}^{\mathrm{T}} \cdot \mathsf{H}$. Hereafter we shall follow the notation and the computational methods developed in [3, 19, 42, 30] (For chromatic polynomials, a related matrix formulation has been discussed in [43, 44, 45, 46].) Concerning notation, no confusion should result between the vertex set V, the variable v, and the vector $\mathbf{v}$. Here $\mathsf{T} = \mathsf{V} \cdot \mathsf{H}$ is the transfer matrix, and H (resp. V) corresponds to adding one more layer of horizontal (resp. vertical) bonds. The matrices T, V, and H act on the space connectivities of sites on the top layer, whose basis elements are indexed $\mathbf{v}_{\mathcal{P}}$ are indexed by partitions $\mathcal{P}$ of the single-layer vertex set $\{1, \ldots, L\}$. In particular, $\mathbf{u}_{\mathrm{id}} = \mathbf{v}_{\{\{1\},\{2\},\ldots,\{L\}\}}$.

To simplify the notation, we shall denote the elements of the basis $\mathbf{v}_{\mathcal{P}}$ by a shorthand using Kronecker delta functions: for instance $\mathbf{v}_{\{\{1,3\},\{2\},\{4,5\}\}}$ will be written $\delta_{1,3}\delta_{4,5}$. We denote the set of basis elements for a given strip as $\mathbf{P} = \{\mathbf{v}_{\mathcal{P}}\}$.

As we are dealing with planar lattices, only non-crossing partitions occur. The number of such partitions is given by the Catalan numbers

$$C_n = \frac{1}{n+1} \binom{2n}{n} \tag{3.2}$$

In the triangular-lattice strip with free boundary conditions there is no additional symmetry that allows us to reduce the number of partitions; thus the dimension of the transfer matrix for width L is [19]

$$N_{Z,\text{tri,FF},L} = C_L \tag{3.3}$$

We have obtained the transfer matrices $\mathsf{T}(L_\text{F})$ and the vectors $\mathbf{w}$ and $\mathbf{u}_\text{id}$ using symbolic computation with MATHEMATICA as in [19, 3]. We have double-checked these results using a different program written in PERL.

An equivalent way to present a general formula for the partition function is via a generating function. Labelling a lattice strip of a given type and width as G_m, with m the length, one has

$$\Gamma(G, q, v, z) = \sum_{m=0}^{\infty} z^m Z(G_m, q, v) \tag{3.4}$$

where $\Gamma(G, q, v, z)$ is a rational function

$$\Gamma(G, q, v, z) = \frac{\mathcal{N}(G, q, v, z)}{\mathcal{D}(G, q, v, z)} \tag{3.5}$$

with

$$\mathcal{N}(G, q, v, z) = \sum_{j=0}^{\deg_z(\mathcal{N})} A_{G,j} z^j \tag{3.6}$$

$$\mathcal{D}(G, q, v, z) = 1 + \sum_{j=1}^{N_{Z,\text{tri,BC},L}} b_{G,j} z^j = \prod_{j=1}^{N_{Z,\text{tri,BC},L}} (1 - \lambda_{G,j} z) \tag{3.7}$$

where the subscript BC denotes the boundary conditions. In the transfer-matrix formalism, the $\lambda_{G,j}$'s in the denominator of the generating function, eq. (3.7), are the eigenvalues of T.

Strips of the triangular lattice are well-defined for widths $L \geq 2$. The partition function $Z(G, q, v)$ has been calculated (for arbitrary q, v, and m) for the strip with $L = 2_\text{F}$ in [4] by two of us using a systematic iterative application of the deletion-contraction theorem. $Z(G, q, v)$ was also studied for arbitrary q and v and zeros calculated for $L = 3, 4$ and various lengths in [5]. Here after reviewing the $L_\text{F} = 2_\text{F}$ case in our formalism, we shall report explicit results for the partition function for $L_\text{F} = 3_\text{F}$. For $4_\text{F} \leq L_\text{F} \leq 6_\text{F}$, the expressions for $\mathsf{T}(L_\text{F})$, $\mathbf{w}(L_\text{F})$ and $\mathbf{u}_\text{id}(L_\text{F})$ are so lengthy that we cannot include them here. They are available from the authors on request and in the MATHEMATICA file `transfer_Tutte_tri.m` which is available with the electronic version of this paper in the `cond-mat` archive at `http://arXiv.org`.

3.1 $L = 2_\text{F}$

Although this partition function was given earlier in [4], it is useful to review the calculation from the point of view of the (spin-representation) transfer matrix. The

number of elements in the basis is equal to $C_2 = 2$: $\mathbf{P} = \{1, \delta_{1,2}\}$. In this basis, the transfer matrices and the other relevant quantities are given by

$$\mathsf{T} = \begin{pmatrix} q^2 + 4qv + 5v^2 + v^3 & (1+v)(q+3v+v^2) \\ v^2(q+3v+v^2) & v^2(1+v)(2+v) \end{pmatrix} \tag{3.8a}$$

$$\mathbf{w}^{\mathsf{T}} = q(q+v, 1+v) \tag{3.8b}$$

$$\mathbf{u}_{\mathrm{id}}^{\mathsf{T}} = (1,0) \tag{3.8c}$$

Because certain expressions recur in transfer matrices for wider strips, it is convenient to re-express (3.8) in terms of these expressions; we have

$$\mathsf{T} = \begin{pmatrix} T_0 & D_1 E_3 \\ v^2 E_3 & v^2 D_1 D_2 \end{pmatrix} \tag{3.9a}$$

$$\mathbf{w}^{\mathsf{T}} = q(F_1, D_1) \tag{3.9b}$$

where

$$D_k = v + k \tag{3.10a}$$

$$F_k = q + kv \tag{3.10b}$$

$$E_k = q^2 + kv + v^2 \tag{3.10c}$$

$$T_0 = q^2 + 4qv + 5v^2 + v^3 \tag{3.10d}$$

In terms of this transfer matrix and these vectors one calculates the partition function $Z(G_m, q, v)$ for the strip with a given length m via eq. (3.1). Equivalently, one can calculate the partition function using a generating function, and this was the way in which the results were presented in [4], with

$$\mathcal{N} = \prod_{j=1}^{2}(1 - \lambda_{tf2,j} z) \tag{3.11}$$

and

$$\lambda_{tf2,(1,2)} = \frac{1}{2}\left[T_{S12} \pm (q + 3v + v^2)\sqrt{R_{S12}}\right] \tag{3.12}$$

where

$$T_{S12} = v^4 + 4v^3 + 7v^2 + 4qv + q^2 \tag{3.13}$$

and

$$R_{S12} = q^2 + 2qv - 2qv^2 + 5v^2 + 2v^3 + v^4 \tag{3.14}$$

The product of these eigenvalues, which is the determinant of T, is

$$\det(\mathsf{T}) = v^2(1+v)^2(v+q)^2 = v^2 D_1^2 F_1^2 \tag{3.15}$$

The vanishing of this determinant at $v = -1$ and $v = -q$ occur because in each case one of the two eigenvalues is absent for, respectively, the chromatic and flow polynomials [47]. Analogous formulas can be given for $\det(\mathsf{T})$ for higher values of L; we omit these for brevity.

3.2 $L = 3_\mathrm{F}$

The number of elements in the basis is equal to $C_3 = 5$: $\mathbf{P} = \{1, \delta_{1,2}, \delta_{1,3}, \delta_{2,3}, \delta_{1,2,3}\}$. In this basis, the transfer matrices and the other relevant quantities are given by

$$
\mathsf{T} = \begin{pmatrix}
T_1 & D_1 F_3 E_3 & T_2 & D_1 T_3 & D_1^2 T_4 \\
v^2 F_3 E_3 & v^2 D_1 D_2 F_2 & v^2 T_5 & v^2 D_1 T_4 & v^2 D_1^2 D_2 \\
v^3 E_3 & v^2 D_1 E_3 & v^2 T_5 & v^3 D_1 D_2 & v^2 D_1^2 D_2 \\
v^2 E_3 E_4 & v^2 D_1 D_2 E_3 & v^2 T_6 & v^2 D_1 D_2 E_4 & v^2 D_1^2 D_2^2 \\
v^4 D_3 E_3 & v^3 D_1 D_2 E_3 & v^3 T_7 & v^4 D_1 D_2 D_3 & v^3 D_1^2 D_2^2
\end{pmatrix}
\tag{3.16a}
$$

$$
\mathbf{w}^\mathrm{T} = q\left(F_1^2, D_1 F_1, E_2, D_1 F_1, D_1^2 \right)
\tag{3.16b}
$$

$$
\mathbf{u}_\mathrm{id}^\mathrm{T} = (1, 0, 0, 0, 0)
\tag{3.16c}
$$

where the T_k are shorthand notations used in this section, defined as

$$
\begin{aligned}
T_1 &= q^3 + 7q^2 v + 19 q v^2 + 19 v^3 + 2 q v^3 + 5 v^4 & \text{(3.17a)} \\
T_2 &= q^2 + 7 q v + 16 v^2 + q v^2 + 9 v^3 + 2 v^4 & \text{(3.17b)} \\
T_3 &= q^2 + 6 q v + 11 v^2 + q v^2 + 4 v^3 & \text{(3.17c)} \\
T_4 &= q + 5 v + 2 v^2 & \text{(3.17d)} \\
T_5 &= q + 6 v + 4 v^2 + v^3 & \text{(3.17e)} \\
T_6 &= 2q + 13 v + 13 v^2 + 6 v^3 + v^4 & \text{(3.17f)} \\
T_7 &= q + 12 v + 13 v^2 + 6 v^3 + v^4 & \text{(3.17g)}
\end{aligned}
$$

4   Potts Model Partition Functions for Triangular-lattice Strips with Cylindrical Boundary Conditions

The Potts model partition function $Z(G, q, v)$ for a triangular-lattice strip of width L vertices and length m vertices with cylindrical boundary conditions can be written as

$$
\begin{aligned}
Z(L_\mathrm{P} \times m_\mathrm{F}, q, v) &= \mathbf{v}^\mathrm{T} \cdot \mathsf{H} \cdot \mathsf{T}^{m-1} \cdot \mathbf{u}_\mathrm{id} & \text{(4.1a)} \\
&= \mathbf{w}^\mathrm{T} \cdot \mathsf{T}^{m-1} \cdot \mathbf{u}_\mathrm{id} & \text{(4.1b)}
\end{aligned}
$$

where again $\mathbf{w}^\mathrm{T} = \mathbf{v}^\mathrm{T} \cdot \mathsf{H}$. Results on $Z(G, q, v)$ for $2_\mathrm{P} \leq L_\mathrm{P} \leq 4_\mathrm{P}$ with cylindrical boundary conditions were previously given in [5]. Here we shall present explicit results for this partition function for strips of the triangular lattice with cylindrical boundary conditions and widths $2_\mathrm{P} \leq L_\mathrm{P} \leq 4_\mathrm{P}$. Results for the transfer matrices in computer-readable files for widths up to $L_\mathrm{P} = 9_\mathrm{P}$ are also available upon request; they are too lengthy to present here.

In the computation of the transfer matrix for a triangular-lattice strip with cylindrical boundary conditions there is a technical complication in order to treat correctly

the last diagonal bond joining columns L and 1 [19, Section 3]. Instead of considering a triangular-lattice strip of width L and cylindrical boundary conditions, we start with a strip of width $L+1$ and free boundary conditions. The parameter v is the same for all edges, except for the vertical edges corresponding to column $L + 1$, where it takes the value $v = 0$. After performing the computation, we identify columns 1 and $L + 1$. This procedure implies that there are double vertical edges (with parameters v and 0) connecting sites on column 1; but their net contribution is v, as expected.

We obtain in this way a transfer matrix of dimension C_{L+1}. This matrix can be simplified by noting that there are many zero eigenvalues. Let us denote by $\{\mathbf{v}_j^{(s)}\}$ (resp. $\{\mathbf{v}_j^{(n)}\}$) the basis elements corresponding to $L + 1$ being (resp. not being) a singleton. The number of elements of $\{\mathbf{v}_j^{(s)}\}$ is C_L; hence the cardinality of $\{\mathbf{v}_j^{(n)}\}$ is $C_{L+1} - C_L$. The zero eigenvalues are associated with certain eigenvectors of the form $\mathbf{v}_1 - \mathbf{v}_2$ where $\mathbf{v}_1 \in \{\mathbf{v}_j^{(s)}\}$ and $\mathbf{v}_2 \in \{\mathbf{v}_j^{(n)}\}$. Let us make the following change of variable

$$\mathbf{v}_i' = \begin{cases} \mathbf{v}_i^{(s)} - \mathbf{v}_j^{(n)} & i = 1, \ldots, C_{L+1} - C_L \\ \mathbf{v}_i^{(s)} & i = C_{L+1} - C_L + 1, \ldots, C_{L+1} \end{cases} \tag{4.2}$$

where the first elements corresponds to eigenvectors with zero eigenvalues, and the last C_L elements are those of the basis $\{\mathbf{v}_j^{(s)}\}$. Then, the transfer matrix takes the simple form

$$\mathsf{T}' = \begin{pmatrix} 0 & \mathsf{T}^{(n)} \\ 0 & \mathsf{T}^{(s)} \end{pmatrix} \tag{4.3}$$

where $\mathsf{T}^{(s)}$ (resp. $T^{(n)}$) is a matrix of dimension C_L (resp. $C_{L+1} - C_L$). In this new basis the vectors $\mathbf{w}$ and $\mathbf{u}_{\mathrm{id}}$ take the form

$$\mathbf{w}' = \left(0, \mathbf{w}^{(s)}\right) \tag{4.4a}$$

$$\mathbf{u}_{\mathrm{id}}' = \left(0, \mathbf{u}_{\mathrm{id}}^{(s)}\right) \tag{4.4b}$$

Thus, we can write the partition function in terms of $\mathsf{T}^{(s)}$, $\mathbf{w}^{(s)}$ and $\mathbf{u}_{\mathrm{id}}^{(s)}$ alone

$$Z(L_{\mathrm{P}} \times m_{\mathrm{F}}, q, v) = \mathbf{w}^{(s)\ \mathrm{T}} \cdot [\mathsf{T}^{(s)}]^{m-1} \cdot \mathbf{u}_{\mathrm{id}}^{(s)} \tag{4.5}$$

So far we have a transfer matrix with the same dimension as for free boundary conditions (namely, $N_{Z,\mathrm{tri,FF},L} = C_L$). We can reduce even more the dimension of the transfer matrix by noting that cylindrical boundary conditions introduce an extra symmetry (i.e. translations along the transverse direction). In particular, we can make a further change of basis in the subspace $\{\mathbf{v}_j^{(s)}\}$ so that

$$\mathbf{v}_i^{(s)\prime} = \begin{cases} \mathbf{v}_i^{(s,n)} & i = 1, \ldots, C_L - N_{Z,\mathrm{tri,PF},L} \\ \mathbf{v}_i^{(s,t)} & i = C_L - N_{Z,\mathrm{tri,PF},L} + 1, \ldots, C_L \end{cases} \tag{4.6}$$

where the last $N_{Z,\mathrm{tri,PF},L}$ (resp. the first $C_L - N_{Z,\mathrm{tri,PF},L}$) elements $\{\mathbf{v}_i^{(s,t)}\}$ (resp. $\{\mathbf{v}_i^{(s,n)}\}$) are translational-invariant (resp. non-translational-invariant) combinations

23

of the original vectors $\{\mathbf{v}_i^{(s)}\}$. In this new basis, the transfer matrix $\mathsf{T}^{(s)}$ takes a block diagonal form

$$\mathsf{T}^{(s)\prime} = \begin{pmatrix} \mathsf{T}^{(s,n)} & 0 \\ 0 & \mathsf{T}^{(s,t)} \end{pmatrix} \tag{4.7}$$

and the vectors $\mathbf{w}^{(s)}$ and $\mathbf{u}_{\mathrm{id}}^{(s)}$ take the form

$$\mathbf{w}^{(s)\prime} = \left(0, \mathbf{w}^{(s,t)} \right) \tag{4.8a}$$

$$\mathbf{u}_{\mathrm{id}}^{(s)\prime} = \left(0, \mathbf{u}_{\mathrm{id}}^{(s,t)} \right) \tag{4.8b}$$

The partition function can be computed using the transfer matrix $\mathsf{T}^{(s,t)}$

$$Z(L_{\mathrm{P}} \times m_{\mathrm{F}}, q, v) = \mathbf{w}^{(s,t)\ \mathrm{T}} \cdot [\mathsf{T}^{(s,t)}]^{m-1} \cdot \mathbf{u}_{\mathrm{id}}^{(s,t)} \tag{4.9}$$

The dimension of $\mathsf{T}^{(s,t)}$ will be denoted by $N_{Z,\mathrm{tri,PF},L}$ and is given by Theorem 2.2 (see also Table 1).

For $L \geq 6$ there is a further simplification, which is also present in the chromatic-polynomial case [30]: in the translation-invariant subspace the transfer matrix does commute with the reflection operation. Thus, we can pass to a new basis consisting of connectivities that are either even or odd under reflection. In this new basis, the transfer matrix $\mathsf{T}^{(s,t)}$ has the block diagonal form

$$\mathsf{T}^{(s,t)\prime} = \begin{pmatrix} \mathsf{T}_-^{(s,t)} & 0 \\ 0 & \mathsf{T}_+^{(s,t)} \end{pmatrix} \tag{4.10}$$

and the vectors $\mathbf{w}^{(s,t)}$ and $\mathbf{u}_{\mathrm{id}}^{(s,t)}$ take the form

$$\mathbf{w}^{(s,t)\prime} = \left(0, \mathbf{w}_+^{(s,t)} \right) \tag{4.11a}$$

$$\mathbf{u}_{\mathrm{id}}^{(s,t)\prime} = \left(0, \mathbf{u}_{\mathrm{id},+}^{(s,t)} \right) \tag{4.11b}$$

Thus, we can compute the partition function using the transfer matrix $\mathsf{T}^{(s,t)\prime}$

$$Z(L_{\mathrm{P}} \times m_{\mathrm{F}}, q, v) = \mathbf{w}_+^{(s,t)\ \mathrm{T}} \cdot [\mathsf{T}_+^{(s,t)}]^{m-1} \cdot \mathbf{u}_{\mathrm{id},+}^{(s,t)} \tag{4.12}$$

In what follows, we shall drop the superindices $^{(st)}$ and the subindex $_+$ to simplify the notation. The dimension of the transfer matrix $\mathsf{T}_+^{(s,t)} \equiv \mathsf{T}$ corresponds to the number of partition classes of the numbers $\{1, 2, \ldots, L\}$ that are invariant under translations and reflections. Thus, this number is precisely $N_{Z,\mathrm{sq,PF},L}$ and is given in terms of L by eq. (2.52) (see Table 1 for some numerical values).

We have obtained the transfer matrices $\mathsf{T}(L_{\mathrm{P}})$ and the vectors $\mathbf{w}(L_{\mathrm{P}})$ and $\mathbf{u}_{\mathrm{id}}(L_{\mathrm{P}})$ using symbolic computation with MATHEMATICA for $L_{\mathrm{P}} \leq 5_{\mathrm{P}}$. For $6_{\mathrm{P}} \leq L_{\mathrm{P}} \leq 9_{\mathrm{P}}$, we have used two different programs (one written in C and the other one in PERL), which were also used to double-check the results for $L \leq 5_{\mathrm{P}}$. For $5_{\mathrm{P}} \leq L \leq 9_{\mathrm{P}}$, the expressions for $\mathsf{T}(L_{\mathrm{P}})$ and the vectors $\mathbf{w}(L_{\mathrm{P}})$ and $\mathbf{u}_{\mathrm{id}}(L_{\mathrm{P}})$ can be found in the MATHEMATICA file `transfer_Tutte_tri.m` which is available with the electronic version of this paper in the `cond-mat` archive at `http://arXiv.org`.

4.1 $L = 2_\mathrm{P}$

The number of elements in the basis is two, with $\mathbf{P} = \{1, \delta_{1,2}\}$; the transfer matrices and the other relevant quantities are given by

$$\mathsf{T} = \begin{pmatrix} q^2 + 6qv + 12v^2 + qv^2 + 8v^3 + 2v^4 & D_1^2(q + 4v + 2v^2) \\ v^2(2q + 12v + 13v^2 + 6v^3 + v^4) & v^2 D_1^2 D_2^2 \end{pmatrix} \quad (4.13\mathrm{a})$$

$$\mathbf{w}^\mathrm{T} = q\left(E_2, D_1^2\right) \quad (4.13\mathrm{b})$$

$$\mathbf{u}_\mathrm{id}^\mathrm{T} = (1, 0) \quad (4.13\mathrm{c})$$

As before, we have used the shorthand notation introduced above (3.10a)/(3.10c).

4.2 $L = 3_\mathrm{P}$

The number of (translational-invariant) elements in the basis is three: $\mathbf{P} = \{1, \delta_{1,2} + \delta_{1,3} + \delta_{2,3}, \delta_{1,2,3}\}$. The transfer matrices and the vectors $\mathbf{w}$ and $\mathbf{u}_\mathrm{id}$ are given by

$$\mathsf{T} = \begin{pmatrix} T_{11} & 3D_1 T_{12} & D_1^3 T_{13} \\ v^2 T_{21} & v^2 D_1 T_{22} & v^2 D_1^3 D_2^2 \\ v^4 D_3 T_{31} & 3v^3 D_1 D_2 T_{32} & v^3 D_1^3 D_2^3 \end{pmatrix} \quad (4.14\mathrm{a})$$

$$\mathbf{w}^\mathrm{T} = q\left(V_1, 3D_1 E_2, D_1^3\right) \quad (4.14\mathrm{b})$$

$$\mathbf{u}_\mathrm{id}^\mathrm{T} = (1, 0, 0) \quad (4.14\mathrm{c})$$

where the factors D_k, E_k are given in (3.10a)/(3.10c), and

$$V_1 = q^2 + 3qv + 3v^2 + 2v^3 \quad (4.15\mathrm{a})$$

$$T_{11} = q^3 + 9q^2 v + 33qv^2 + 4qv^3 + 50v^3 + 21v^4 + 3v^5 \quad (4.15\mathrm{b})$$

$$T_{12} = q^2 + 8qv + 20v^2 + 2qv^2 + 14v^3 + 3v^4 \quad (4.15\mathrm{c})$$

$$T_{13} = q + 6v + 3v^2 \quad (4.15\mathrm{d})$$

$$T_{21} = q^2 + 10qv + 30v^2 + 2qv^2 + 22v^3 + 7v^4 + v^5 \quad (4.15\mathrm{e})$$

$$T_{22} = 6q + 38v + 2qv + 42v^2 + 18v^3 + 3v^4 \quad (4.15\mathrm{f})$$

$$T_{31} = 3q + 18v + 15v^2 + 6v^3 + v^4 \quad (4.15\mathrm{g})$$

$$T_{32} = q + 12v + 13v^2 + 6v^3 + v^4 \quad (4.15\mathrm{h})$$

4.3 $L = 4_\mathrm{P}$

The number of (translational-invariant) elements in the basis is six: $\mathbf{P} = \{1, \delta_{1,2} + \delta_{2,3} + \delta_{3,4} + \delta_{1,4}, \delta_{1,3} + \delta_{2,4}, \delta_{1,2,3} + \delta_{1,2,4} + \delta_{1,3,4} + \delta_{2,3,4}, \delta_{1,2,3,4}, \delta_{1,4}\delta_{2,3} + \delta_{1,2}\delta_{3,4}\}$. The transfer matrix is given by

$$\mathsf{T} = \quad (4.16)$$

$$
\begin{pmatrix}
T_{11} & 4D_1 T_{12} & 2E_4 T_{13} & 4D_1^2 T_{14} & D_1^4 T_{15} & 2D_1^2 T_{16} \\
v^2 T_{21} & 2v^2 D_1 T_{22} & v^2 T_{23} & v^2 D_1^2 T_{24} & v^2 D_1^4 D_2^2 & 2v^2 D_1^2 D_2 T_{26} \\
v^3 T_{31} & 2v^2 D_1 T_{32} & 4v^2 T_{34}^2 & 4v^2 D_1^2 D_2 T_{34} & v^2 D_1^4 D_2^2 & v^2 D_1^2 T_{36} \\
v^4 D_3 T_{41} & v^3 D_1 T_{42} & 2v^3 T_{34} T_{54} & 2v^3 D_1^2 D_2 T_{44} & v^3 D_1^4 D_2^3 & v^3 D_1^2 D_2 T_{46} \\
v^6 D_3^2 T_{51} & 4v^5 D_1 D_2 D_3 T_{52} & 2v^4 T_{54}^2 & 4v^4 D_1^2 D_2^2 T_{54} & v^4 D_1^4 D_2^4 & 2v^5 D_1^2 D_2^2 D_3 T_{56} \\
v^4 T_{62}^2 & 4v^4 D_1 D_2 T_{62} & v^4 T_{63} & 2v^4 D_1^2 D_2^2 & 0 & 2v^4 D_1^2 D_2^2
\end{pmatrix}
$$

where the factors $D_k(v)$ and E_k are defined in (3.10a)/(3.10c); the T_{ij} are given by

$$
\begin{aligned}
T_{11} &= q^4 + 12q^3 v + 62q^2 v^2 + 164qv^3 + 4q^2 v^3 + 192v^4 + 29qv^4 \\
&\quad + 72v^5 + 6v^6 \tag{4.17a}
\end{aligned}
$$

$$
T_{12} = q^3 + 11q^2 v + 47qv^2 + q^2 v^2 + 80v^3 + 11qv^3 + 40v^4 + 5v^5 \tag{4.17b}
$$

$$
T_{13} = q^2 + 8qv + 24v^2 + qv^2 + 16v^3 + 4v^4 \tag{4.17c}
$$

$$
T_{14} = q^2 + 10qv + 28v^2 + 3qv^2 + 20v^3 + 4v^4 \tag{4.17d}
$$

$$
T_{15} = q + 8v + 4v^2 \tag{4.17e}
$$

$$
T_{16} = q^2 + 10qv + 32v^2 + 3qv^2 + 24v^3 + 5v^4 \tag{4.17f}
$$

$$
\begin{aligned}
T_{21} &= q^3 + 12q^2 v + 54qv^2 + 2q^2 v^2 + 96v^3 + 18qv^3 + 59v^4 + qv^4 \\
&\quad + 12v^5 + v^6 \tag{4.17g}
\end{aligned}
$$

$$
T_{22} = 3q^2 + 28qv + q^2 v + 80v^2 + 13qv^2 + 65v^3 + qv^3 + 18v^4 + 2v^5 \tag{4.17h}
$$

$$
\begin{aligned}
T_{23} &= 3q^2 + 34qv + 96v^2 + 23qv^2 + 120v^3 + 8qv^3 + 67v^4 + qv^4 \\
&\quad + 18v^5 + 2v^6 \tag{4.17i}
\end{aligned}
$$

$$
T_{24} = 10q + 56v + 6qv + 63v^2 + qv^2 + 26v^3 + 4v^4 \tag{4.17j}
$$

$$
T_{26} = q + 8v + 5v^2 + v^3 \tag{4.17k}
$$

$$
T_{31} = 2q^2 + 18qv + 48v^2 + 4qv^2 + 31v^3 + 8v^4 + v^5 \tag{4.17l}
$$

$$
T_{32} = q^2 + 14qv + 52v^2 + 4qv^2 + 43v^3 + 14v^4 + 2v^5 \tag{4.17m}
$$

$$
T_{34} = q + 6v + 4v^2 + v^3 \tag{4.17n}
$$

$$
T_{36} = 2q + 24v + 27v^2 + 12v^3 + 2v^4 \tag{4.17o}
$$

$$
T_{41} = q^2 + 11qv + 36v^2 + 2qv^2 + 24v^3 + 7v^4 + v^5 \tag{4.17p}
$$

$$
\begin{aligned}
T_{42} &= 2q^2 + 43qv + q^2 v + 216v^2 + 28qv^2 + 270v^3 + 4qv^3 + 138v^4 \\
&\quad + 36v^5 + 4v^6 \tag{4.17q}
\end{aligned}
$$

$$
T_{44} = 3q + 24v + qv + 27v^2 + 12v^3 + 2v^4 \tag{4.17r}
$$

$$
T_{46} = q + 24v + 27v^2 + 12v^3 + 2v^4 \tag{4.17s}
$$

$$
T_{51} = 4q + 24v + 17v^2 + 6v^3 + v^4 \tag{4.17t}
$$

$$
T_{52} = 2q + 18v + 15v^2 + 6v^3 + v^4 \tag{4.17u}
$$

$$
T_{54} = q + 12v + 13v^2 + 6v^3 + v^4 \tag{4.17v}
$$

$$
T_{56} = 4 + 3v + v^2 \tag{4.17w}
$$

$$
T_{62} = q + 6v + 2v^2 \tag{4.17x}
$$

$$
T_{63} = 3q + 24v + 26v^2 + 12v^3 + 2v^4 \tag{4.17y}
$$

The vectors $\mathbf{w}$ and $\mathbf{u}_{\mathrm{id}}$ are given by

$$
\begin{align}
\mathbf{w}^{\mathrm{T}} &= q\left(V_1, 4D_1V_2, 2E_2^2, 4D_1^2E_2, D_1^4, 2D_1^2E_2\right) \tag{4.18a}\\
\mathbf{u}_{\mathrm{id}}^{\mathrm{T}} &= (1, 0, 0, 0, 0, 0) \tag{4.18b}
\end{align}
$$

where

$$
\begin{align}
V_1 &= q^3 + 4q^2v + 6qv^2 + 4v^3 + v^4 \tag{4.19a}\\
V_2 &= q^2 + 3qv + 3v^2 + v^3 \tag{4.19b}
\end{align}
$$

5 Partition Function Zeros in the q Plane

In this section we shall present results for zeros and continuous accumulation sets $\mathcal{B}_q$ (in the q-plane) for the partition function of the Potts antiferromagnet on triangular-lattice strips of widths $L \leq 5$ with free or cylindrical boundary conditions.

In Figure 1 we show the partition-function zeros in the q-plane for strips of sizes $L_{\mathrm{F}} \times (10L)_{\mathrm{F}}$ with $2 \leq L \leq 5$ and free boundary conditions. We also show the corresponding limiting curves $\mathcal{B}_q(L, v)$ for the infinite-length limit. Figure 1(a) displays the zeros for $v = -1$ (i.e., the chromatic zeros [48, 51, 30]), and Figures 1(b)–(d) display the corresponding zeros for the non-zero temperatures $v = -0.75$ (b), $v = -0.5$ (c), and $v = -0.25$ (d). The case $L = 2$ was studied in [4] and the cases $L = 3, 4$ were studied in [5, Figs. 3.15, 3.22] for arbitrary temperature, and our zeros are in agreement with these earlier works.

The corresponding partition-function zeros and accumulation sets for triangular-lattice strips with cylindrical boundary conditions are shown in Figure 2. Again, Figure 2(a)–(d) displays the zeros for $v = -1$ (a), $v = -0.75$ (b), $v = -0.5$ (c), and $v = -0.25$ (d). The cases $L = 3, 4$ were studied previously in (Figs. 3.19, 3.25 of) [5] for arbitrary temperature, and our zeros are in agreement with this work.

The case $v = -1$, which is the zero-temperature Potts antiferromagnet (chromatic polynomial) has been previously studied in [48, 50, 51, 19, 30] for the free longitudinal boundary conditions and in [52, 53, 51, 54, 20] for periodic longitudinal boundary conditions. For the case of free longitudinal boundary conditions [30] contains results for $L \leq 9_{\mathrm{F}}$ and $L \leq 12_{\mathrm{P}}$. Our Figures 1(a) and 2(a) include calculations up to $L = 5$ for comparison with other values of v. Although some curves, such as those for cylindrical boundary conditions, may enclose regions, the curves do not enclose regions containing the origin. One observes that for either type of transverse boundary condition, as the width L increases, the left-hand arc endpoints move slowly toward the origin. When this was observed in earlier work for several different lattice strips, [48], it motivated the suggestion that in the limit $L \to \infty$ for strips with free longitudinal boundary conditions, the limiting $\mathcal{B}_q$ would separate the q plane into regions including a curve passing through $q = 0$ [48, 17]. The specific calculation of $\mathcal{B}_q(v = -1)$ in the limit $L \to \infty$ reported by Baxter [46] has this feature. (For critical comments on certain features of Baxter's results, see the detailed discussion in [30].) The property that $\mathcal{B}_q$ separates the q plane into regions with one of the curves on $\mathcal{B}_q$ passing

through the origin is also observed for lattice strips with finite width L if one imposes periodic longitudinal boundary conditions [55, 56, 52, 53, 57, 58, 51, 54, 59].

In making inferences about possible $L \to \infty$ characteristics of the continuous accumulation set of zeros $\mathcal{B}(G_s, L \times \infty)$ in the q or v plane for infinite-length, width-L lattice strip graphs of type G_s, one should recall that, in general, $\lim_{L \to \infty} \mathcal{B}(G_s, L \times \infty)$ is different from the continuous accumulation set of the zeros of the partition function for the usual 2D thermodynamic limit defined by starting with an $L_y \times L_x$ section of a regular lattice and letting L_x and L_y both approach infinity with L_y/L_x a finite nonzero constant. This type of noncommutativity was encountered in previous studies of $\mathcal{B}$ for the Potts model free energy on infinite-length, finite-width strips with periodic longitudinal boundary conditions [18, 4, 23, 22]; for these strips, $\mathcal{B}$ is noncompact in the v plane, reflecting the fact that the Potts model has a ferromagnetic critical point only at $T = 0$ (i.e. $K = \infty$, hence $v = \infty$) for any width L, no matter how great, whereas for the 2D lattice defined in the thermodynamic limit, it has a ferromagnetic critical point at a finite temperature, so $\mathcal{B}$ is compact in the v plane. Noncommutativity of this type was also found in studies of $\mathcal{B}_q$. For example, in calculations of $\mathcal{B}_q$ for infinite-length strips of the triangular lattice with cyclic boundary conditions, it was found that this locus always passes through $q = 2$ [52, 53, 51, 54], whereas, in contrast, the locus found in [46] for the infinite-width limit of strips with cylindrical boundary conditions does not pass through $q = 2$. Similarly, in calculations of $\mathcal{B}_q$ for infinite-length strips of the square lattice with cyclic boundary conditions, it was found that this locus always passes through $q = 2$, whereas in calculations of $\mathcal{B}_q$ for infinite-length strips of the square lattice with cylindrical boundary conditions [50, 19, 59, 42], it was found that $\mathcal{B}$ does not pass through $q = 2$, strongly suggesting that this difference will persist in the limit $L_y \to \infty$.

At nonzero temperature for the antiferromagnet, as represented in our figures by the range $-0.75 \leq v \leq -0.25$, the partition-function zeros in the q-plane have a different shape: as L increases, the limiting curves $\mathcal{B}_q(L, v)$ tend to a bean-shaped curve or set of arcs, open on the left, without substantial protruding branches, in contrast to many of the $v = -1$ curves. For a given value of v in the range considered, as the width L increases, the curve envelope moves outward somewhat and the arc endpoints on the left move slowly toward $q = 0$. This behavior is consistent with the hypotheses that for a given v, as $L \to \infty$, (i) $\mathcal{B}_q$ would approach a limiting locus as $L \to \infty$ and (ii) this locus would separate the q plane into different regions, with a curve passing through $q = 0$ as well as a maximal real value, $q_c(v)$. This is qualitatively the same type of behavior that was found earlier for the square-lattice strips [18, 23, 3]. In particular, our results are consistent with the inference that as $L \to \infty$, $\mathcal{B}_q$ for $v = -1$ would pass through $q_c(v = -1) = 4$, corresponding to the property that the $q = 4$ Potts antiferromagnet has a zero-temperature critical point on the (infinite) triangular lattice [60].

For a given L, as v increases from -1 to 0, i.e., as the inverse temperature β decreases from infinity to 0 for the antiferromagnet, the zeros and the limiting curve contract to a point at $q = 0$. This is an elementary consequence of the fact that these lattice strips have fixed maximal vertex degree and as the parameter $K = \beta J$

approaches zero, the spin-spin interaction term in $\mathcal{H}$, eq. (1.2), vanishes, so that the sum over states just counts all q possible spin states independently at each vertex, and $Z(G, q, v)$ approaches the value $Z(G, q, 0) = q^n$. An upper bound on the magnitudes of the zeros is given by the following theorem by Sokal:

Theorem 5.1 *(Sokal [61]) Let $G = \{V, E\}$ be a loopless finite undirected graph of maximum degree $\leq r$, equipped with complex edge weights $\{v_e\}_{e \in E}$ satisfying $|1+v_e| \leq 1$ for all e. Let $|v|_{\max} = \max_{e \in E} |v_e|$. Then all the zeros of $Z(G, q, \{v_e\})$ lie in the disc $|q| < C(r)v_{\max}$ with $C(r) \leq 7.963907r$.*

This is a loose bound; for all of the strips with cylindrical boundary conditions and for the free strips with widths $L \geq 3$, the maximal degree is $r = 6$, so that the above theorem implies that $|q| \lesssim 47.8|v|_{\max}$. Thus, for example, for $v = -1$, this reads $|q| \lesssim 47.8$, whereas in fact $|q| \lesssim 4$ for free boundary conditions and $|q| \lesssim 4.5$ for cylindrical boundary conditions. A general feature is that the limiting curves and associated zeros tend to be located mostly in the $\text{Re}(q) \geq$ half plane.

As noted, it is evident in Figures 1 and 2 that as L increases, the accumulation set $\mathcal{B}_q(L, v)$ moves outwards. As expected, the convergence to the limit $L \to \infty$ seems to be faster with cylindrical boundary conditions, as there are no surface effects when the length is made infinite.

One can also plot $\mathcal{B}_q$ for the ferromagnetic region $0 \leq v \leq \infty$ (e.g., Figs. 2 and 13 of [4]). Although we have not included these plots here, we note that an elementary Peierls argument shows that the q-state Potts ferromagnet on infinite-length, finite-width strips has no finite-temperature phase transition and associated magnetic long range order. Hence, for this model $\mathcal{B}_q$ does not cross the positive real q axis for $0 \leq v < \infty$.

6 Partition Function Zeros in the v Plane

6.1 General

In this section we shall present results for zeros and continuous accumulation sets $\mathcal{B}_v$ (in the v-plane) for the partition function of the Potts antiferromagnet on triangular-lattice strips of widths $L \leq 5$ and free or cylindrical boundary conditions. Our results hold for arbitrarily great length L and for any real or complex value of q; they thus complement calculations of the Potts model partition function for fixed positive integer values of q on sections of the triangular lattice [62, 63, 64, 65]. We shall focus here on integer values of q, since these are the most relevant from a physical point of view. We recall the possible noncommutativity in the definition of the free energy for certain integer values of q (see eqs. (2.10), (2.11) of [18] or (1.17) of [4]): $\lim_{n \to \infty} \lim_{q \to q_s} Z(G, q, v)^{1/n} \neq \lim_{q \to q_s} \lim_{n \to \infty} Z(G, q, v)^{1/n}$ As discussed in [18], because of this noncommutativity, the formal definition (1.4) is, in general, insufficient to define the free energy f at these special points q_s; it is necessary to specify the order of the limits that one uses in the above equation. We denote the two definitions using different orders of limits as f_{qn} and f_{nq}: $f_{nq}(\{G\}, q, v) = \lim_{n \to \infty} \lim_{q \to q_s} n^{-1} \ln Z(G, q, v)$ and $f_{qn}(\{G\}, q, v) = \lim_{q \to q_s} \lim_{n \to \infty} n^{-1} \ln Z(G, q, v)$.

As a consequence of this noncommutativity, it follows that for the special set of points $q = q_s$ one must distinguish between (i) $(\mathcal{B}_v(\{G\}, q_s))_{nq}$, the continuous accumulation set of the zeros of $Z(G, q, v)$ obtained by first setting $q = q_s$ and then taking $n \to \infty$, and (ii) $(\mathcal{B}_v(\{G\}, q_s))_{qn}$, the continuous accumulation set of the zeros of $Z(G, q, v)$ obtained by first taking $n \to \infty$, and then taking $q \to q_s$. For these special points (cf. eq. (2.12) of [18]),

$$(\mathcal{B}_v(\{G\}, q_s))_{nq} \neq (\mathcal{B}_v(\{G\}, q_s))_{qn} \tag{6.1}$$

Here this noncommutativity will be relevant for $q = 0$ and $q = 1$.

In Figures 3–7 we show the partition-functions zeros in the v-plane (for a fixed value of q) for strips of sizes $L_\text{F} \times (10L)_\text{F}$ with $2 \leq L \leq 5$ and free boundary conditions. We also show the corresponding limiting curves $\mathcal{B}_v(L, q)$ for the limit of infinite strip length. For simplicity, we have displayed each value of L on a different plot: $L = 2$ (a), $L = 3$ (b), $L = 4$ (c), and $L = 5$ (d). The corresponding partition-function zeros and accumulation sets for triangular-lattice strips with cylindrical boundary conditions are shown in Figures 8–12 with the same notation as for the former figures. Complex-temperature phase diagrams and associated partition function zeros were given in [4] for $L = 2$ for free and periodic longitudinal boundary conditions and free transverse boundary conditions. Results for $L = 4_\text{F}$ and $L = 4_\text{P}$ at zero and finite temperatures were given before in [5]. Our present calculations are in agreement with, and extend, this previous work.

On the infinite triangular lattice (defined via the 2D thermodynamic limit as given above), the phase transition point separating the paramagnetic (PM) and ferromagnetic (FM) phases is determined as the (unique) real positive solution of the equation [67]

$$v^3 + 3v^2 - q = 0 \tag{6.2}$$

In previous studies such as [18, 4], it has been found that although infinite-length, finite-width strips are quasi-one-dimensional systems and hence the Potts model has no physical finite-temperature transition on such systems, some aspects of the complex-temperature phase diagram have close connections with those on the (infinite) triangular lattice. We shall discuss some of these connections below.

6.2 $q = 0$

From the cluster representation of $Z(G, q, v)$, eq. (1.5), it follows that this partition function has an overall factor of $q^{k(G)}$, where $k(G)$ denotes the number of components of G, i.e., an overall factor of q for a connected graph. Hence, $Z(G, q = 0, v) = 0$. In the transfer matrix formalism, this is evident from the overall factor of q coming from the vector $\mathbf{w}$. However, if we first take the limit $n \to \infty$ to define $\mathcal{B}$ for $q \neq 0$ and then let $q \to 0$ or, equivalently, extract the factor q from the left vector $\mathbf{w}$, we obtain a nontrivial locus, namely $(\mathcal{B}_v(\{G\}, 0)_{qn}$. This is a consequence of the noncommutativity (6.1) for $q = 0$.

With the second order of limits or the equivalent removal of the factor of q in Z, we obtain the locus $\mathcal{B}_v(q = 0)$ shown in Figures 3 (free boundary conditions)

and 8 (cylindrical boundary conditions). The accumulation set $\mathcal{B}_v(L, q = 0)$ seems to converge to a roughly circular curve. We see in Figures 3 and 8 that the limiting curves cross the real v-axis at $v \approx -3$. We note the interesting feature that this is a root of eq. (6.2) for $q = 0$. For the case of cylindrical boundary conditions, $\mathcal{B}_v(q = 0)$ includes a small line segment on the real axis near $v = -3$, with a length that decreases as L increases. As L increases, the arc endpoints on the upper and lower right move toward the real axis. It is possible that these could pinch this axis at $v = 0$ as $L \to \infty$, corresponding to the other root of (6.2) for $q = 0$.

6.3 $q = 1$

For $q = 1$, the spin-spin interaction in (1.2) always has the Kronecker delta function equal to unity, and hence the Potts model partition function is trivially given by

$$Z(G, q = 1, v) = e^{K|E|} = (1 + v)^{|E|} \tag{6.3}$$

where $|E|$ is the number of edges in the graph G. This has a single zero at $v = -1$. But again, one encounters the noncommutativity (6.1) for $q = 1$. It is interesting to analyze this in terms of the transfer matrix formalism. At this value of q, both the transfer matrix and the left vector $\mathbf{w}$ are non-trivial. There is thus a cancellation of terms that yields the result (6.3). The case $L = 2_P$ is the simplest one to analyze: the eigenvalues and coefficients for $q = 1$ are given by

$$\lambda_1(1, v) = 2v^2 ; \qquad c_1(1, 0) = 0 \tag{6.4a}$$
$$\lambda_2(1, v) = (1 + v)^6 ; \quad c_2(1, 0) = (1 + v)^2 \tag{6.4b}$$

Thus, only the second eigenvalue contributes to the partition function, and it gives the expected result $Z(2_P \times m_F, q = 1, v) = (1 + v)^{6m-4}$. For $L = 2_F$ we obtain:

$$\lambda_1(1, v) = v^2 ; \qquad c_1(1, 0) = 0 \tag{6.5a}$$
$$\lambda_2(1, v) = (1 + v)^4 ; \quad c_2(1, 0) = (1 + v) \tag{6.5b}$$

giving rise to $Z(2_F \times m_F, q = 1, v) = (1 + v)^{4m-3}$. The case $L = 3_P$ is similar: there is a single eigenvalue $\lambda_1(1, v) = (1 + v)^9$ with a non-zero coefficient $c_1(1, v) = (1 + v)^3$, and the other two eigenvalues [which are the roots of $x^2 - xv^2(3v^3 + 13v^2 + 24v + 3) + v^5(1 + v)(6 + 5v + 6v^2)$] have identically zero coefficients $c_{2,3}(1, v) = 0$. Thus, the partition function takes the form $Z(3_P \times m_F, q = 1, v) = (1 + v)^{9m-6} = (1 + v)^{|E|}$.

In general, we conclude that at $q = 1$ only the eigenvalue $\lambda = (1 + v)^{3L_P}$ (resp. $\lambda = (1 + v)^{3L_F - 2}$) contributes to the partition function for cylindrical (resp. free) boundary conditions, and its coefficient is $c = (1 + v)^{L_P}$ (resp. $c = (1 + v)^{L_F - 1}$). The other eigenvalues do not contribute as they have zero coefficients. This is the analogue of what was found for the strips with cyclic boundary conditions, where the various λ's fall into sets $\lambda_{G,d,j}$ such that all of the λ's with a fixed d have a unique coefficient which is a polynomial of degree d in q given by [18, 4, 20]

$$c^{(d)} = U_{2d}\left(\frac{\sqrt{q}}{2}\right) = \sum_{j=0}^{d} (-1)^j \binom{2d - j}{j} q^{d-j} \tag{6.6}$$

31

where $U_\nu(z)$ is the Chebyshev polynomial of the second kind. These coefficients vanish at certain values of q, which means that if one evaluates the partition function first at these values and then takes the limit $n \to \infty$, the corresponding λ's will not contribute to Z, while if one takes $n \to \infty$ first, calculates the free energy and the locus $\mathcal{B}_{qn}$, and then sets q equal to one of these values, the λ's will, in general contribute. In particular, we recall (eq. (2.18) of [20]) that if $q = 1$, then $c^{(d)}$ vanishes if $d = 1 \mod 3$. Thus, we see similar manifestations of the noncommutativity (6.1) for strips with free and periodic boundary conditions.

In our present case, in order to obtain $\mathcal{B}_{qn}$, we have computed the Tutte-polynomial zeros and the corresponding limiting curves for $q = 0.999$ (see Figures 4 and 9). The accumulation sets $\mathcal{B}_v(L, q = 0.999)$ for $L = 2_F$ to $L = 5_F$ consists of arcs that come close to forming an almost closed bean-shaped curve, with an involution on the right that deepens as L increases. Solving the $q = 1$ special case of eq. (6.2) yields the roots $v = -2.879385..$, $v = -0.652703...$, and $v = 0.5320888...$ The locus $\mathcal{B}_v$ crosses the real v axis at two points, and our results are consistent with the inference that as $L \to \infty$, these two crossing points are the first two roots listed above. For free boundary conditions with width $L = 3, 4, 5$, $\mathcal{B}_{qn}$ exhibits a small involution on the left. A noteworthy feature of this locus is that it is relatively smooth, without the prongs that tend to occur for the other values of q discussed here.

6.4 $q = 2$

The zeros and accumulation sets for $q = 2$ are displayed in Figures 5 and 10 for free and cylindrical boundary conditions. Fig. 5(a) contains the same information as Fig. 4 of [4] (which is plotted in a different temperature variable, a^{-1}). The finite-size effects for the accumulation sets $\mathcal{B}_v(L, q = 2)$ are noticeably larger for free, in comparison with cylindrical, boundary conditions, as expected. In the latter case, the curves $\mathcal{B}_v(L, q = 2)$ for $L = 2, 3, 4, 5$ fall very approximately one on top of the preceding one. For cylindrical boundary conditions, we see that the curve $\mathcal{B}_v(L, q = 2)$ is symmetric under the replacement $a \to -a$. The reason for this is that in this case all of the vertices except for the end-vertices, which constitute a vanishingly small fraction in the limit of infinite length, are equivalent (i.e., the graph is r-regular) and have even degree r. In general, this property applies for the complex-temperature phase diagram of the $q = 2$ (Ising) special case of the Potts model for an infinite lattice where the coordination number is even [68, 69, 70]. Our strips with free transverse boundary conditions are not r-regular graphs because the vertices on the upper and lower sides have a different degree than those in the interior. Because of this, the $\mathcal{B}_v$ in this case does not have the $a \to -a$ symmetry. From previous work [18, 4] one knows that the loci $\mathcal{B}_v$ are different for strips with free or periodic transverse boundary conditions and free longitudinal boundary conditions, on the one hand, and free or periodic transverse boundary conditions and periodic (or twisted periodic) longitudinal boundary conditions. One anticipates, however, that in the limit of infinite width, the subset of the complex-temperature phase diagram that is relevant to real physical thermodynamics will be independent of the boundary conditions used to obtain the 2D thermodynamic limit.

In the 2D thermodynamic limit, one knows the complex-temperature phase diagram exactly for the $q = 2$ (Ising) case. (This isomorphism involves the redefinition of the spin-spin exchange constant $J_{\mathrm{Potts}} = 2J_{\mathrm{Ising}}$ and hence $K_{\mathrm{Potts}} = 2K_{\mathrm{Ising}}$, where K_{Potts} is denoted simply K here.) The simplest way to portray the complex-temperature phase diagram is in the a^2 or $u = a^{-2}$ plane since this automatically incorporates the $a \to -a$ symmetry noted above. In the u plane, the complex-temperature phase diagram, with boundaries given by $\mathcal{B}_u$, is (see Fig. 1(a) of [70] which is equivalent, by duality to the complex-temperature phase diagram for the honeycomb lattice given as Fig. 2 in [72])

$$\mathcal{B}_u : \quad \{|u + \frac{1}{3}| = \frac{2}{3}\} \quad \cup \quad \{-\infty \le u \le -\frac{1}{3}\} \tag{6.7}$$

i.e., the union of a circle centered at $u = -1/3$ with radius $2/3$ and the semi-infinite line segment extending leftward from $u = -1/3$ along the real u axis. In the a^{-1} plane (Fig. 1(b) of [70], related by duality to Fig. 3 of [72]), $\mathcal{B}$ is the union of a vertically elongated oval crossing the real axis at $\pm 1/\sqrt{3}$, the imaginary a^{-1} axis at $\pm i$, and two semi-infinite line segments extending from $i/\sqrt{3}$ to $i\infty$ and from $-i/\sqrt{3}$ to $-i\infty$ along the imaginary axis. Equivalently, in the a plane, $\mathcal{B}$ is the union of a horizontally elongated oval crossing the real a axis at $\pm\sqrt{3}$ and the imaginary a axis at $\pm i$, and a line segment along the imaginary axis extending between $\sqrt{3}i$ and $-\sqrt{3}i$. The locus $\mathcal{B}_v$ in the v plane is obtained from this by translation by one unit, since $v = a - 1$. This locus separates the complex v plane into three phases: (i) the paramagnetic phase, including the infinite-temperature point $v = 0$, where the S_q symmetry is realized explicitly (S_q being the symmetric group on q numbers, the symmetry group of the Hamiltonian), (ii) the ferromagnetic phase, including the real interval $v_c(q = 2) \le v \le \infty$ where the S_q symmetry is spontaneously broken by the existence of a nonzero magnetization, and (iii) an unphysical phase (denoted "O" for "other" in [70]) including the point $v = -2$. Here

$$a_c(q = 2) = v_c(q = 2) + 1 = \sqrt{3} \tag{6.8}$$

is the physical critical point separating the PM and FM phases (for a review of the Ising model on the triangular lattice, see, e.g., [73]) . These physical PM and FM phases have complex-temperature extensions off the real v axis. The PM and O phases are separated by the subset of the vertical line segment extending between $a = i$ and $a = -i$; this line segment terminates at the points $a = \pm\sqrt{3}i$. Because of the maximal frustration, there is no antiferromagnetic phase at finite temperature. The presence of a zero-temperature critical point in the 2D Ising antiferromagnet [74] is manifested by the fact that $\mathcal{B}_v$ passes through $v = -1$, i.e., $a = 0$ (as part of the above-mentioned vertical line segment). The complex-temperature phase boundary $\mathcal{B}_v$ crosses the real v axis at $v = \sqrt{3} - 1$, separating the FM and PM phases, at $v = -1$, separating the PM and O phases, and at $v = -1 - \sqrt{3}$, separating the O and (complex-temperature analytic continuation of the) FM phases. In [4] the $\mathcal{B}$ for an infinite-length free or cyclic strip with width $L = 2$ were compared with this 2D phase diagram. These three points, $v = -1, -1 \pm \sqrt{3}$, are the three roots of the $q = 2$ special case of eq. (6.2).

Using our exact results, we can compare our loci $\mathcal{B}_v$ for a wide variety of widths and either free or periodic transverse boundary conditions with the known complex-temperature phase diagram for the Ising model on the infinite 2D triangular lattice. This comparison is simplest for the case of cylindrical boundary conditions, so we concentrate on these results. For the finite values of L that we have considered, $\mathcal{B}_v$ has the form of two complex-conjugate arcs that cross two complex-conjugate line segments on the imaginary axis at $v = -1 \pm i$. One sees that as L increases, the endpoints of the arcs move down toward the real axis, as do the endpoints of the line segments. As $L \to \infty$, we expect that these arc endpoints will close, forming the above-mentioned horizontally elongated oval and vertical line segment extending from $v = -1 + \sqrt{3}i$ to $v = -1 - \sqrt{3}i$ that constitute the complex-temperature phase boundaries $\mathcal{B}$ for the Ising model on the infinite triangular lattice.

6.5 $q = 3$

In contrast to the $q = 2$ case, the free energy of the q-state Potts model has not been calculated exactly for $q \geq 3$ on any 2D (or higher-dimensional) lattice and hence the complex-temperature phase diagrams are not known exactly. The $q = 3$ special case of eq. (6.2) has the root

$$v_{PM-FM,q=3} \equiv v_c(q = 3) = -1 + \cos(2\pi/9) + \sqrt{3}\sin(2\pi/9) = 0.879385... \quad (6.9)$$

corresponding to the physical PM-FM phase transition point, and two other roots at the complex-temperature values

$$v = -1 + \cos(2\pi/9) - \sqrt{3}\sin(2\pi/9) = -1.347296... \quad (6.10)$$

and

$$v = -1 - 2\cos(2\pi/9) = -2.532089... \quad (6.11)$$

Discussions of the complex-temperature solutions of eq. (6.2) and their connections with the complex-temperature phase diagram have been given in [62, 63, 64, 65]. A number of studies involving exact calculation of the partition function for various q values on large sections of the triangular lattice have been performed [62, 63, 64, 65]. (There have also been many studies calculating zeros for the Potts model with $q \geq 3$ on the square lattice; see [3] for references to these works.)

The zeros and accumulation sets for $q = 3$ are displayed in Figures 6 and 11 for free and cylindrical boundary conditions. We expect that the pair of complex-conjugate endpoints in this regime will eventually converge to the ferromagnetic critical point $v_c(q = 3)$ as $L \to \infty$. However, obviously, an infinite-length strip of finite width L is a quasi-one-dimensional system, so the Potts model has no physical finite-temperature phase transition on such a strip for any finite L.

In the antiferromagnetic regime $-1 \leq v < 0$, we observe noticeable finite-size effects even with cylindrical boundary conditions. In this regime, we also observe a complex-conjugate pair of endpoints with small value of $\text{Im}(v)$ that, as $L \to \infty$, are expected to approach the real v axis at the transition point separating the param-agnetic and antiferromagnetic (AFM) phases of the $q = 3$ Potts antiferromagnet on

the infinite triangular lattice. Monte Carlo and series analyses [75, 76, 77, 78] have yielded the conclusion that the PM-AFM transition in the $q = 3$ Potts antiferromagnet on the triangular lattice is weakly first-order. A high-accuracy determination of the location of the PM-AFM transition temperature T was obtained in [78] by means of Monte Carlo simulations: $T = 0.62731 \pm 0.00006$, or equivalently

$$v_{PM-AFM,q=3} = -0.79691 \pm 0.00003 \tag{6.12}$$

We shall improve this estimate below.

Finally, in the complex-temperature interval $v < -1$, the finite-size and boundary condition effects are evidently very strong. Because of this, in previous work, a combination of partition-function zeros and analyses of low-temperature series expansions was used [65]; these enable one at least to locate some points on the complex-temperature phase boundary. As regards the infinite 2D triangular lattice, because of a duality relation, the complete physical temperature interval $0 \leq T \leq \infty$, i.e., $0 \leq a \leq 1$ of the q-state Potts antiferromagnet on the honeycomb lattice is mapped to the complex-temperature interval $-\infty \leq v \leq -q)$ on the triangular lattice (and vice versa) [63]. As was noted in [63], it follows that because the $q = 3$ Potts antiferromagnet on the honeycomb lattice is disordered for all temperatures, including $T = 0$, the free energy for this model on the triangular lattice is analytic in the interval $-\infty < v \leq -3$, and hence no part of the complex-temperature phase boundary $\mathcal{B}_v$ can cross the negative real axis in this interval. In particular, one anticipates that as $L \to \infty$ for the infinite-length, width-L strips, the left-most arcs on $\mathcal{B}_v$ will not close and pinch the negative real axis in this interval. Our calculations of $\mathcal{B}_v$ are consistent with the inference that as $L \to \infty$, this locus crosses the real axis at the points (6.10) and (6.11), although there are significant differences between the loci obtained with free and cylindrical boundary conditions.

We also observe certain line segments on the real v axis in the complex-temperature region. We note that massless phases with algebraic decays of correlation functions have been suggested for the Potts model on the (infinite) square lattice at real values of v and q in the intervals $-2 - \sqrt{4-q} \leq v \leq -2 + \sqrt{4-q}$ with $q \in (0, 4)$ and $q \neq B_r = 4\cos^2(\pi/r)$, and it was conjectured that these might also occur for other 2D lattices [66]. However, the correspondence of these suggestions with our results is not clear; for example, the above interval suggested in [66] shrinks to zero as $q \to 4$, but we observe clear line segments on the real v axis for $q = 4$ for both free and cylindrical boundary conditions (see Figs. 7 and 12). A possible physical subset of the above range of v given in [66] would be the antiferromagnet interval $-1 \leq v < 0$. However, the condition that $q \neq B_r$ excludes all of the integral values of q in the indicated range (recall that $B_2 = 0$, $B_3 = 1$, $B_4 = 2$, $B_6 = 3$, and $B_1 = \lim_{n\to\infty} B_n = 4$). The claim in [66] is thus complicated by the fact that although it is possible formally to define the Potts model partition function $Z(G, q, v)$ using (1.5) for real positive non-integral q for the antiferromagnetic case, $-1 \leq v < 0$, here the model does not satisfy the usual statistical mechanical requirement that the partition function is positive, and hence does not, in general, admit a Gibbs measure [71, 18]. This leads to pathologies that preclude a physical interpretation, such as negative partition function, negative specific heat, and non-existence of a $|V| \to \infty$ limit for thermodynamic functions that

35

is independent of boundary conditions [71, 18, 4]. As regards the connection with the locus $\mathcal{B}$, a signal of a massless phase would be a line segment on $\mathcal{B}$ on the real v axis for fixed q or the real q axis for fixed v. For the zero-temperature Potts antiferromagnet, i.e., chromatic polynomial, $v = -1$, these phases would thus occur in the intervals between the Beraha numbers, $0 < q < 1$, $1 < q < 2$, $2 < q < (1/2)(3 + \sqrt{5})$, and so forth. However, it has been proved that there are no real zeros of a chromatic polynomial in the intervals $-\infty < q < 0$, $0 < q < 1$, and $1 < q \leq 32/27$ [79, 80]. Since $\mathcal{B}$ forms as an accumulation set of zeros, this makes it difficult to see how there could be a line segments in these intervals, in particular, the intervals $0 < q < 1$ and $1 < q \leq 32/27$. Again, it is not clear how to reconcile the results of these theorems with a suggestion that there would be massless phases with associated real line segments on $\mathcal{B}$ in these intervals.

6.6 $q = 4$

For $q = 4$, eq. (6.2) has the physical root

$$v_{PM-FM,q=4} \equiv v_c(q = 4) = 1 \tag{6.13}$$

corresponding to the PM-FM phase transition point and a double root at the complex-temperature point

$$v = -2 \tag{6.14}$$

The zeros and accumulation sets for $q = 4$ are displayed in Figures 7 and 12. One observes the approach of the right-most complex-conjugate arcs to the real axis as L increases, i.e. the approach to the PM-FM critical point in this case. For a given L, the approach to the exactly known value $v_{PM-FM,q=4} = 1$ in eq. (6.13) is closer for cylindrical versus free boundary conditions, as is anticipated since the former minimize boundary effects. The $q = 4$ Potts antiferromagnet on the triangular lattice has a zero-temperature critical point, so that $v = -1$ is on $\mathcal{B}_v$ [60] (this is not a root of eq. (6.2)). For $L \geq 2$ for free boundary conditions and for $L \geq 2$ for cylindrical boundary conditions, we see how a pair of complex-conjugate arc endpoints approaches the real axis as L increases, consistent with the inference that these would pinch at $v = -1$ in the $L \to \infty$ limit. For both free and cylindrical boundary conditions and various values of L, one sees that $\mathcal{B}_v$ contains an intersection point at the complex-temperature value $v = -2$, in agreement with the expectation from eq. (6.14). The fact that the $q = 4$ Potts antiferromagnet is disordered on the honeycomb lattice for all temperatures T including $T = 0$ implies that $\mathcal{B}_v$ does not cross the negative real axis in the interval $-\infty < v \leq -4$ [63]. In particular, this implies that as $L \to \infty$, the leftmost arc endpoints on $\mathcal{B}_v$ in the figures do not move down to pinch the negative real axis in this interval $-\infty < v \leq -4$, provided that the limit $L \to \infty$ of these infinite-length, width-L strips commutes with the 2D thermodynamic limit for the triangular lattice as regards this aspect of the complex-temperature phase diagram.

We do not show plots for $q \geq 5$, but recall that the Potts antiferromagnet is expected to be disordered (with exponential decay of spin-spin correlation functions) even at $T = 0$ on the triangular lattice. This can be proved rigorously for $q \geq 11$ as

36

a slight improvement of the result that q-state Potts antiferromagnet is disordered at all temperatures on a lattice with coordination number r if $q > 2r$ [71]. The property that the Potts antiferromagnet is disordered at all T on the triangular lattice for $q \geq 5$ is reflected in the property that $\mathcal{B}_v$ does not pass through $v = -1$.

7 Internal Energy and Specific Heat

The partition function (1.1) can be used to derive the free-energy density $f(G, q, v)$

$$f(G, q, v) = \frac{1}{|V|} \log Z(G, q, v) \tag{7.1}$$

for finite $|V|$, with the $V \to \infty$ limit having been defined in eq. (1.4) above. The internal energy E and the specific heat C are derived in the usual way from the free energy as

$$E(G, q, v) = -J\frac{\partial f}{\partial K} = -J(v + 1)\frac{\partial f}{\partial v} \tag{7.2}$$

and

$$C = \frac{\partial E}{\partial T} = k_B K^2 (v + 1) \left[\frac{\partial f}{\partial v} + (v + 1)\frac{\partial^2 f}{\partial v^2} \right] \equiv k_B K^2 C_H \tag{7.3}$$

Henceforth, for convenience, we shall use a definition of E without the factor $-J$ in (7.2), and we shall use the dimensionless function C_H in discussions of the specific heat. Let us suppose that G is a triangular-lattice strip graph of size $L \times m$. In the limit $m \to \infty$, since only the dominant eigenvalue $\lambda_d(q, v)$ of the transfer matrix contributes to the free energy, one has

$$f(q, v; L) = \frac{1}{L} \log \lambda_d \tag{7.4a}$$

$$E(q, v; L) = \frac{1}{L} \Lambda_1 \tag{7.4b}$$

$$C_H(q, v; L) = \frac{1}{L} \left[\Lambda_2 + \Lambda_1 - \Lambda_1^2 \right] \tag{7.4c}$$

where the $\Lambda_i(q, v; L)$ are defined by

$$\Lambda_i(q, v; L) = \frac{(1 + v)^i}{\lambda_d(q, v; L)} \frac{\partial^i \lambda_d}{\partial v^i} \tag{7.5}$$

The infinite-length limits of the triangular-strips considered here are quasi-one-dimensional systems with analytic free energies at all temperatures. Hence the dominant eigenvalue λ_d is the same on the whole semi-axis $\mathrm{Im}(v) = 0$, $\mathrm{Re}(v) \geq -1$. Furthermore, as discussed in [18], the free energy and its derivatives with respect to the temperature are independent of the longitudinal boundary conditions in the limit $m \to \infty$ (although they depend on the transverse boundary conditions).

In Figure 13 we have plotted the internal energy E (7.2), the specific heat C_H (7.3), and the Binder cumulant U_4 (7.11) (see below) for $q = 3$ on a triangular-lattice strip of width up to $L = 6$ and infinite length with cylindrical boundary conditions.

The behavior of the energy for the triangular-lattice strips with cylindrical boundary conditions is interesting: the curves cross each others close to the critical value v_c in the ferromagnetic regime. In particular, for $q = 2$ we find that all curves cross at $v_c(2) = \sqrt{3} - 1 \approx 0.7320508....$ For $q = 3, 4$ we find that the crossings are close to the respective PM-FM critical points $v_c(3)$ given exactly in eq. (6.9) ($= 0.8793852...$) and $v_c(4) = 1$, but they do not coincide precisely with these critical points. The reason for the above behavior is the following: the triangular-lattice Potts model on a triangular lattice at a given value of the temperature Boltzmann variable v is related by duality to the hexagonal-lattice Potts model at a different temperature variable

$$v' = \frac{q}{v} \tag{7.6}$$

This relation is exact when the original triangular-lattice is defined on an infinitely long cylinder of width L. In the Ising case $q = 2$, there is an additional transformation (namely, the star-triangle transformation) that maps back the hexagonal-lattice Potts model onto a triangular-lattice Potts model at temperature variable $v''(v)$. This transformation allows us to compute the critical temperature v_c (i.e., v_c is the unique fixed point of the equation $v''(v) = v$) and the critical energy $E_c = E(q, v_c; L)$. When we perform the computation of E_c in the limit $m \to \infty$, all finite-size corrections disappear, so that [81]

$$E_c(q = 2; L) \equiv E(q = 2, v_c; L) = E_c(q = 2; \infty) = \frac{5}{2} \tag{7.7}$$

However, for $q \neq 2$ there is no star-triangle transformation, and this implies the existence of corrections to scaling:

$$E_c(q; L) \equiv E(q, v_c; L) = E_c(q; \infty) + \sum_{k=1}^{\infty} \frac{A_k}{L^{\omega_k}} , \qquad q \neq 2 \tag{7.8}$$

where the parameters $\{\omega_k(q)\}$ are correction-to-scaling exponents that depend in general on the value of q.

One can obtain a pseudo-critical temperature $v_E \equiv v_E(q, L, L')$ by solving the equation

$$E(q, v_E, L) = E(q, v_E, L') \tag{7.9}$$

When $L, L' \to \infty$, we expect that this quantity will converge to the true critical value $v_c(q)$. This method has been employed in the the literature to locate critical points for several statistical-mechanical systems [82, 83, and references therein].

Another pseudo-critical temperature can be obtained by looking at the point $v_C \equiv v_C(q, L)$ where the specific heat $C(q, v; L)$ attains a maximum value. This value differs from the bulk critical value $v_c(q)$ by finite-size-corrections of order $\sim L^{-1/\nu}$ [84].

We can also consider higher derivatives of the free energy with respect to K. In particular, the quantity $\bar{u}_4$ is the fourth derivative of the free energy with respect to K and, in the limit $m \to \infty$ it can be written as

$$\bar{u}_4(q, v; L) = \frac{\partial^4 f}{\partial K^4} \tag{7.10}$$

Instead of $\bar{u}_4$, it is more useful to deal with the phenomenological quantity U_4 (also called the Binder cumulant [85]) defined as

$$U_4(q, v; L) = \frac{1}{L^2} \frac{\bar{u}_4}{C^2} \tag{7.11}$$

(Since this involves the energy instead of the magnetization, one could also consider a third cumulant.) A plot of this quantity for $q = 3$ is given in Figure 13(c). A third pseudo-critical temperature $v_U \equiv v_U(q, L)$ can be defined as the value at which the Binder cumulant (7.11) attains a minimum value. Again, this estimate is expect to differ from the bulk critical temperature $v_c(q)$ by terms of order $L^{-1/\nu}$ [84].

The computation of the transfer matrices for triangular-lattice strips of width L allows us to compute these three pseudo-critical temperatures (namely, $v_E(q, L, L')$, $v_C(q, L)$, and $v_U(q, L)$). We have computed these estimates for several values of $1/2 \leq q \leq 4$ in the ferromagnetic regime for strips with cylindrical boundary conditions. We expect a finite-size behavior of these three pseudo-critical temperatures of the type

$$v_Q(q; L) = v_c(q) + \sum_{k=1}^{\infty} \frac{A_{Q,k}}{L^{\omega_k}} \tag{7.12}$$

where $Q = E, C, U$, and the $\{A_{Q,k}, \omega_k\}$ are correction-to-scaling amplitudes and exponents, respectively. These quantities depend in general on q. We can try to estimate the critical temperature $v_c(q)$ by fitting the data to the above Ansatz (7.12) with only the leading correction-to-scaling term included

$$v_Q(q; L) = v_c(q) + A_Q L^{-\Delta_Q} \tag{7.13}$$

Although the exact phase transition temperature for the q-state Potts ferromagnet is known, it is useful to compare these pseudo-critical temperature with the exactly known values for the infinite lattice, since we do not know, *a priori*, which estimate v_Q will give the most accurate results. It is important to perform a comprehensive check of the method before studying a phase transition whose critical temperature is not known (for instance, the 3-state triangular-lattice Potts antiferromagnet; see below). We have done this and have found that the estimates coming from the pseudo-critical temperature v_E are better by far than the other two; and the estimate v_U is more accurate than v_C. More precisely, the difference between the extrapolated value for v_c and the exact value is $\sim 10^{-7}$ for v_E for all the $1.5 \leq q \leq 4$ values considered. However, for v_U the discrepancy is of order $\sim 10^{-5}$ for $q \gtrsim 1.5$ and $\sim 10^{-2}$ to 10^{-4} for $q \lesssim 1$. Finally, for v_C the discrepancy is $\sim 10^{-4}$ for $q \gtrsim 2$, and $\sim 10^{-3}$ for $1 \lesssim q \lesssim 1.5$. In conclusion, we can establish the position of the ferromagnetic critical temperature $v_c(q)$ (over the whole range of values of q) by using the pseudo-critical temperature $v_E(L, L')$. The results for v_C and v_U are at least two orders of magnitudes worse, and the accuracy also depends on the value of q: it worsens for $q \lesssim 2$ for v_C, and for $q \lesssim 1.5$ for v_U.

One can try to extend the previous analysis to the antiferromagnetic regime. In Table 2 we show the estimates for the critical temperature of the 3-state Potts antiferromagnet using strips with cylindrical boundary conditions and widths that are

multiples of 3. This constraint is due to the $(\mathrm{mod}\,3)$-oscillations that appear in antiferromagnets: in Figure 13 we clearly observe such oscillations in the antiferromagnetic regime. Thus, we keep only the data with $L = 3, 6, 9, 12$ that is expected to be closer to the thermodynamic limit.[1] (When L is not a multiple of 3, the corresponding triangular-lattice strip with cylindrical boundary conditions is not tripartite, unlike those strips with L a multiple of 3 or the infinite triangular lattice; recall our earlier discussion of the chromatic number for these strips.) The value quoted on the row labelled "MC" comes from the Monte-Carlo study by Adler *et al.* [78]. For $L = 12$ we just list the estimate from the energy crossing since this is superior to the other two estimates, and this gives the value

$$v_c(q = 3) = -0.796927(20) \tag{7.14}$$

The error bar quoted in (7.14) was roughly estimated by comparing the above result to the value of $v_c(q = 3)$ obtained by fitting the data points $v_E(L, L')$ with $L = 3, 6, 9$ and $L' = L + 3$, namely, $v_c(q = 3) = -0.796907$. This is indeed a very conservative estimate for this error bar. Our results in (7.14) is in agreement with, and more accurate than, the estimate from [78] listed above in eq. (6.12).

Acknowledgment

---

[1] To compute the estimates $v_E(q = 3, L, L')$ we need the transfer matrices $\mathsf{T}(L_\mathrm{P}, q = 3)$. For $L_\mathrm{P} \leq 9$, we have used the symbolic transfer matrices of section 4 evaluated at $q = 3$. For larger widths (i.e., $L = 12, 15$), we have computed numerically the corresponding transfer matrices at the particular value $q = 3$.

References

[1] R. B. Potts, Proc. Camb. Phil. Soc. **48**, 106 (1952).

[2] F. Y. Wu, Rev. Mod. Phys. **54**, 235 (1982).

[3] S.-C. Chang, J. Salas, and R. Shrock, J. Stat. Phys. **107** 1207-1253 (2002), cond-mat/0108144.

[4] S.-C. Chang and R. Shrock, Physica **A 286**, 189 (2000), cond-mat/0004181.

[5] H. Kluepfel, Stony Brook thesis "The q-State Potts Model: Partition Functions and Their Zeros in the Complex Temperature and q Planes" (July, 1999); H. Kluepfel and R. Shrock, unpublished.

[6] P. W. Kasteleyn and C. M. Fortuin, J. Phys. Soc. Jpn. **26**, 11 (1969) (Suppl.).

[7] C. M. Fortuin and P. W. Kasteleyn, Physica **57**, 536 (1972).

[8] G. D. Birkhoff, Ann. Math. **14**, 42 (1912).

[9] W. T. Tutte, Can. J. Math. **6**, 80 (1954).

[10] W. T. Tutte, J. Combin. Theory **2**, 301 (1967).

[11] W. T. Tutte, "Chromials", in Lecture Notes in Math. v. 411 (1974) 243; *Graph Theory*, vol. 21 of Encyclopedia of Mathematics and Applications (Addison-Wesley, Menlo Park, 1984).

[12] H. Whitney, Bull. Amer. Math. Soc. **38**, 572 (1932).

[13] F. Y. Wu, J. Stat. Phys. **52**, 99 (1988).

[14] N. L. Biggs, *Algebraic Graph Theory* (2nd ed., Cambridge Univ. Press, Cambridge, 1993).

[15] D. J. A. Welsh, *Complexity: Knots, Colourings, and Counting*, London Math. Soc. Lect. Note Ser. 186 (Cambridge University Press, Cambridge, 1993).

[16] B. Bollobás, *Modern Graph Theory* (Springer, New York, 1998).

[17] R. Shrock, in the *Proceedings of the 1999 British Combinatorial Conference, BCC99* (July, 1999), Discrete Math. **231**, 421 (2001), cond-mat/9908387.

[18] R. Shrock, Physica A **283**, 388 (2000), cond-mat/0001389.

[19] J. Salas and A. Sokal, J. Stat. Phys., **104**, 609 (2001), cond-mat/0004330.

[20] S.-C. Chang and R. Shrock, Physica A **296**, 131 (2001), cond-mat/0005232.

[21] S.-C. Chang and R. Shrock, Int. J. Mod. Phys. B **15**, 443 (2001), cond-mat/0007505.

[22] S.-C. Chang and R. Shrock, Physica A **296**, 183 (2001), cond-mat/0008477.

[23] S.-C. Chang and R. Shrock, Physica A **296**, 234 (2001), cond-mat/0011503.

[24] S.-Y. Kim and R. Creswick, Phys. Rev. **E63**, 066107 (2001), cond-mat/0102090.

[25] S.-C. Chang and R. Shrock, Physica A **301**, 301 (2001), cond-mat/0106607.

[26] S.-C. Chang and R. Shrock, Phys. Rev. E **64**, 066116 (2001), cond-mat/0107012.

[27] N. L. Biggs, R. M. Damerell, and D. A. Sands, J. Combin. Theory B **12**, 123 (1972).

[28] R. C. Read, J. Combin. Theory **4**, 52 (1968).

[29] R. C. Read and W. T. Tutte, "Chromatic Polynomials", in *Selected Topics in Graph Theory, 3*, eds. L. W. Beineke and R. J. Wilson (Academic Press, New York, 1988.).

[30] J.L. Jacobsen, J. Salas, and A.D. Sokal, J. Stat. Phys. **112**, 921 (2003), cond-mat/0204587.

[31] M. E. Fisher, *Lectures in Theoretical Physics* (Univ. of Colorado Press, 1965), vol. 7C, p. 1.

[32] R. Abe, Prog. Theor. Phys. **38**, 322 (1967).

[33] S. Katsura, Prog. Theor. Phys. **38**, 1415 (1967).

[34] S. Ono, Y. Karaki, M. Suzuki, and C. Kawabata, J. Phys. Soc. Jpn. **25**, 54 (1968).

[35] S. Beraha, J. Kahane, and N. Weiss, J. Combin. Theory B **27**, 1 (1979); *ibid.* **28**, 52 (1980).

[36] S.-C. Chang, "Exact results for q-state Potts model partition functions", Ph.D. thesis, State Univ. of New York at Stony Brook (May, 2002).

[37] N. J. A. Sloane, *The On-Line Encyclopedia of Integer Sequences*. Published electronically at `http://www.research.att.com/~njas/sequences/` .

[38] R. P. Stanley, *Enumerative Combinatorics* (Cambridge University Press, Cambridge, 1999), v. 2.

[39] M. Bernstein and N. J. A. Sloane, Linear Algebra and Its Applications **226–228**, 57 (1995). Erratum **320**, 210 (2000).

[40] T. Motzkin, Bull. Amer. Math. Soc. **54**, 352 (1948).

[41] R. Donaghey and L. W. Shapiro, J. Combin. Theory, A **23**, 291 (1977).

[42] J.L. Jacobsen and J. Salas, J. Stat. Phys. **104**, 701 (2001), cond-mat/0011456.

[43] N. L. Biggs, Bull. London Math. Soc. **9**, 54 (1977).

[44] N. L. Biggs, Combin. Theory B **82**, 19 (2001).

[45] R. J. Baxter, J. Phys. A **19**, 2821 (1986).

[46] R. J. Baxter, J. Phys. A **20**, 5241 (1987).

[47] S.-C. Chang and R. Shrock, J. Stat. Phys. **112**, 815 (2003), cond-mat/0205424.

[48] M. Roček, R. Shrock, and S.-H. Tsai, Physica **A252**, 505 (1998)., cond-mat/9712148

[49] R. Shrock and S.-H. Tsai, Physica **A259**, 315 (1998), cond-mat/9807105

[50] M. Roček, R. Shrock, and S.-H. Tsai, Physica **A259**, 367 (1998), 9807106.

[51] S.-C. Chang and R. Shrock, Ann. Phys. **290**, 124 (2001), cond-mat/0004129.

[52] R. Shrock and S.-H. Tsai, Phys. Rev. **E60**, 3512 (1999), cond-mat/9910377.

[53] R. Shrock and S.-H. Tsai, Physica A **275**, 429 (2000), cond-mat/9907403.

[54] S.-C. Chang and R. Shrock, Physica A **292**, 307 (2001), cond-mat/0007491.

[55] R. Shrock and S.-H. Tsai, Phys. Rev. **E55**, 5165 (1997), cond-mat/9612249.

[56] R. Shrock and S.-H. Tsai, J. Phys. A Letts. **32**, L195 (1999), cond-mat/9903233.

[57] R. Shrock, Phys. Lett. **A261**, 57 (1999), cond-mat/9908323.

[58] N. L. Biggs and R. Shrock, J. Phys. A (Letts) **32**, L489 (1999), cond-mat/0001407.

[59] S.-C. Chang and R. Shrock, Physica A **290**, 402 (2001), cond-mat/0004161.

[60] R. J. Baxter, J. Math. Phys. **11**, 784 (1970).

[61] A.D. Sokal, Combin. Prob. Comput. **10**, 41 (2001), cond-mat/9904146.

[62] P. P. Martin and J.-M. Maillard, J. Phys. A **19**, L547 (1986).

[63] H. Feldmann, R. Shrock, and S.-H. Tsai, J. Phys. A (Lett.) **30**, L663 (1997), cond-mat/9710018.

[64] H. Feldmann, R. Shrock, and S.-H. Tsai, J.Phys. Rev. **E57**, 1335 (1998), cond-mat/9711058.

[65] H. Feldmann, A. J. Guttmann, I. Jensen, R. Shrock, and S.-H. Tsai, J. Phys. A **31**, 2287 (1998), cond-mat/9801305.

[66] H. Saleur, Commun. Math. Phys. **132**, 657 (1990); Nucl. Phys. **B360**, 219-263 (1991).

[67] D. Kim and R. Joseph, J. Phys. C **7**, L167 (1974).

[68] V. Matveev and R. Shrock, J. Phys. A **28**, 1557 (1995), hep-lat/9408020.

[69] V. Matveev and R. Shrock, J. Phys. A **28**, 5235 (1995), hep-lat/9503005.

[70] V. Matveev and R. Shrock, J. Phys. A **29**, 803 (1996), hep-lat/9411023.

[71] J. Salas and A. Sokal, J. Stat. Phys. **86**, 551 (1997), cond-mat/9603068; A. Sokal, private communication.

[72] R. Abe, T. Dotera, and T. Ogawa, Prog. Theor. Phys. **85**, 509 (1991).

[73] Domb, C. 1960 *Adv. in Phys.* **9** 149.

[74] J. Stephenson, J. Math. Phys. **5**, 1009 (1964) and references therein.

[75] G. S. Grest, J. Phys. A **14**, L217 (1981).

[76] Y. Saito, J. Phys. A **15**, 1885 (1982).

[77] E. G. Enting and F. Y. Wu, J. Stat. Phys. **28**, 351 (1982).

[78] J. Adler, A. Brandt, W. Janke, and S. Shmulyian, J. Phys. A **28**, 5117 (1995).

[79] B. Jackson, Combin. Prob. Comput. **2**, 325 (1993).

[80] V. Thomassen, Combin. Prob. Comput. **6**, 497 (1997).

[81] J. Salas, J. Phys. A **35**, 1833 (2002), cond-mat/0110287.

[82] M.A. Yurishchev, Nucl. Phys. B (Proc. Suppl.) **83-84**, 727 (2000), hep-lat/9908019.

[83] M.A. Yurishchev, Nucl. Phys. B (Proc. Suppl.) **106**, 917 (2002), hep-lat/0109025.

[84] M.N. Barber, in *Phase Transitions and Critical Phenomena*, Vol. 8, edited by C. Domb and J.L. Lebowitz (Academic Press, New York, 1983).

[85] M.S.S. Challa, D.P. Landau and K. Binder, Phys. Rev. B **34**, 1841 (1986).

L	$N_{Z,\text{tri,FF},L}$	C_{L+1}	$N_{Z,\text{tri,PF},L}$	$N_{Z,\text{sq,PF},L}$
1	1	2	1	1
2	2	5	2	2
3	5	14	3	3
4	14	42	6	6
5	42	132	10	10
6	132	429	28	24
7	429	1430	63	49
8	1430	4862	190	130
9	4862	16796	546	336
10	16796	58786	1708	980
11	58786	208012	5346	2904
12	208012	742900	17428	9176

Table 1: Dimensions of the transfer matrix for triangular-lattice strips. For each strip width L we give the dimension of the transfer matrix for free boundary conditions $N_{Z,\text{tri,FF},L}$ (which is equal to the Catalan number C_L), the dimension of the full transfer matrix for cylindrical boundary conditions (which is C_{L+1}), the dimension for cylindrical boundary conditions when translational symmetry is taken into account $N_{Z,\text{tri,PF},L}$, and the dimension when we project onto the subspace of reflection-invariant connectivities $N_{Z,\text{sq,PF},L}$.

q	L	v_C	v_U	L'	v_E
3	3	-0.7537129688	-0.7746989054	6	-0.7984897326
	6	-0.7916555922	-0.7942230532	9	-0.7971540641
	9	-0.7952008646	-0.7959971452	12	-0.7969905288
	12			15	-0.7969527708
	∞	-0.79660	-0.79668		-0.796927(20)
	MC	-0.79691(3)	-0.79691(3)		-0.79691(3)

Table 2: Pseudo-critical temperatures for the 3-state Potts model in the antiferro-magnetic regime. For each value of the strip width $L = 3k$, we show the pseudo-critical temperatures v_C, v_U, and v_E computed on strips with cylindrical boundary conditions. The row labelled "MC" shows the Monte Carlo estimate for $v_c(q)$.
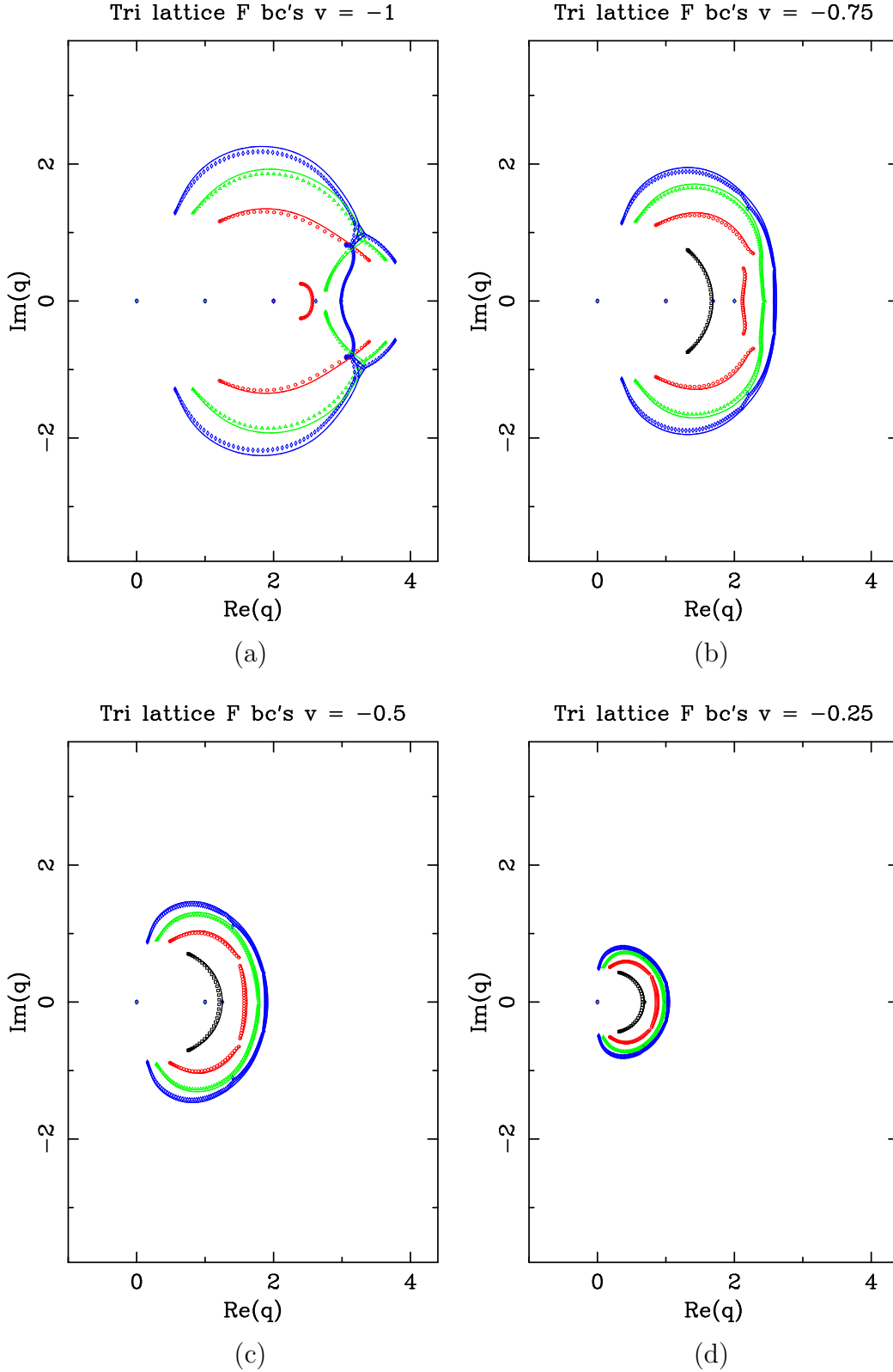
Figure 1: Limiting curves forming the singular locus $\mathcal{B}_q$ for the Potts model free energy for (a) $v = -1$, (b) $v = -3/4$, (c) $v = -1/2$, and (d) $v = -1/4$ on strips with free boundary conditions and several widths L: 2 (black), 3 (red), 4 (green), and 5 (blue). We also show the partition-function zeros for the strips $L_F \times (10L)_F$ for the same values of L: 2 ($\square$, black), 3 ($\circ$, red), 4 ($\triangle$, green), and 5 ($\diamond$, blue). Where the results for $2 \leq L \leq 4$ overlap with those in [4, 5] (see also [48, 51, 30] for $v = -1$), they agree and are included here for comparison.
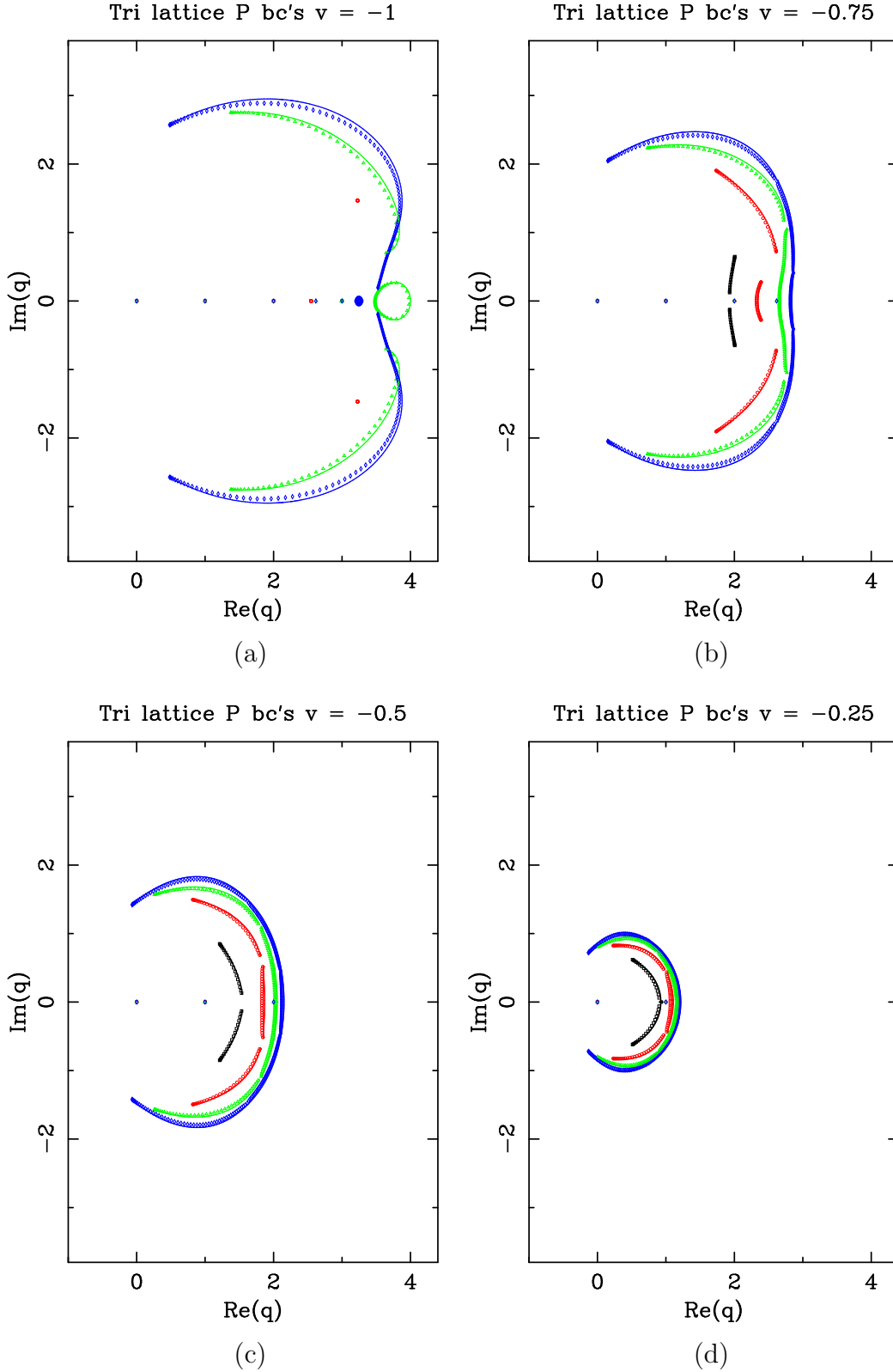
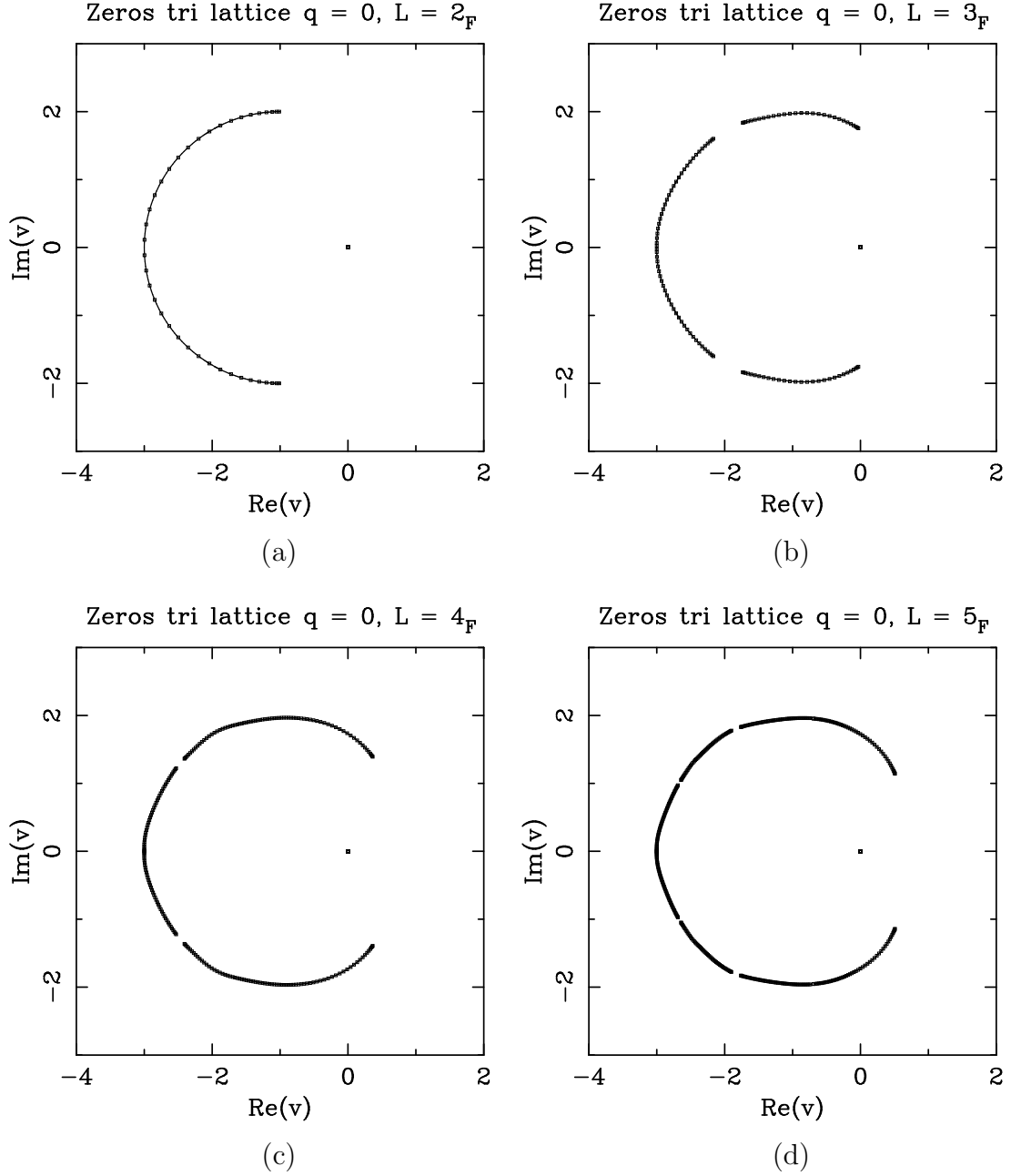Figure 2: Limiting curves forming the singular locus $\mathcal{B}_q$ for the Potts model free energy for (a) $v = -1$, (b) $v = -3/4$, (c) $v = -1/2$, and (d) $v = -1/4$ on strips with cylindrical boundary conditions and several widths L: 2 (black), 3 (red), 4 (green), and 5 (blue). We also show the partition-function zeros for the strips $L_P \times (10L)_F$ for the same values of L. The symbols are as in Figure 1. Where the results for $2 \le L \le 4$ overlap with those in [4, 5] and for $v = -1$ (see also [50, 51, 30] for $3 \le L \le 5$), they agree and are included here for comparison.

Figure 3: Limiting curves forming the singular locus $\mathcal{B}$, in the v plane, for the free energy, defined with the order f_{qn}, of the Potts model for $q = 0$ on the $L_{\mathrm{F}} \times \infty_{\mathrm{F}}$ triangular-lattice strips with (a) $L = 2$, (b) $L = 3$, (c) $L = 4$, and (d) $L = 5$. We also show the zeros of $Z(G, 0, v)/q$ corresponding to the strips $L_{\mathrm{F}} \times (10L)_{\mathrm{F}}$ for each value of L.

49

Zeros tri lattice q = 0.999, L = 2$_F$

Zeros tri lattice q = 0.999, L = 3$_F$

(a)

(b)

Zeros tri lattice q = 0.999, L = 4$_F$
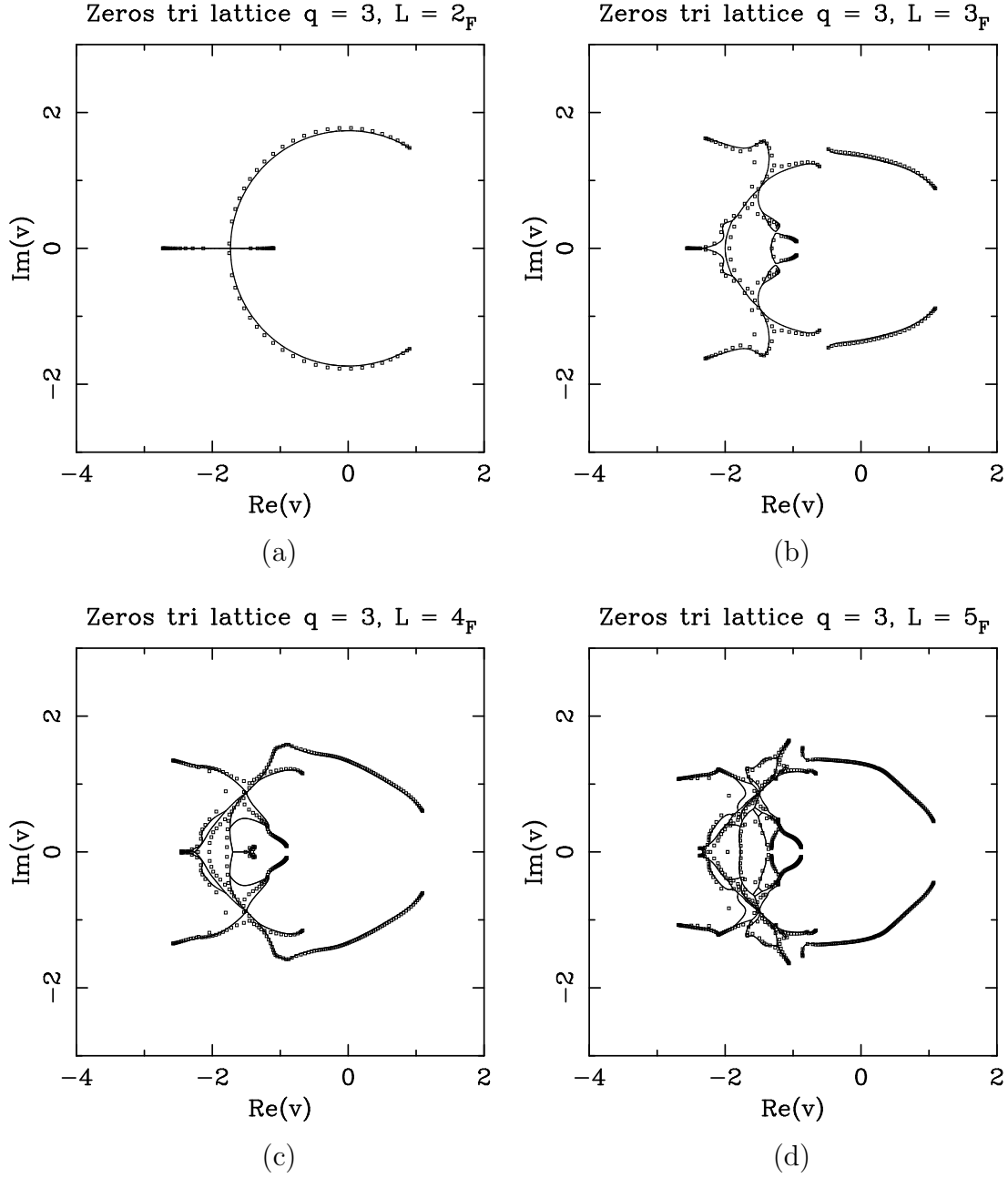
Zeros tri lattice q = 0.999, L = 5$_F$

(c)

(d)
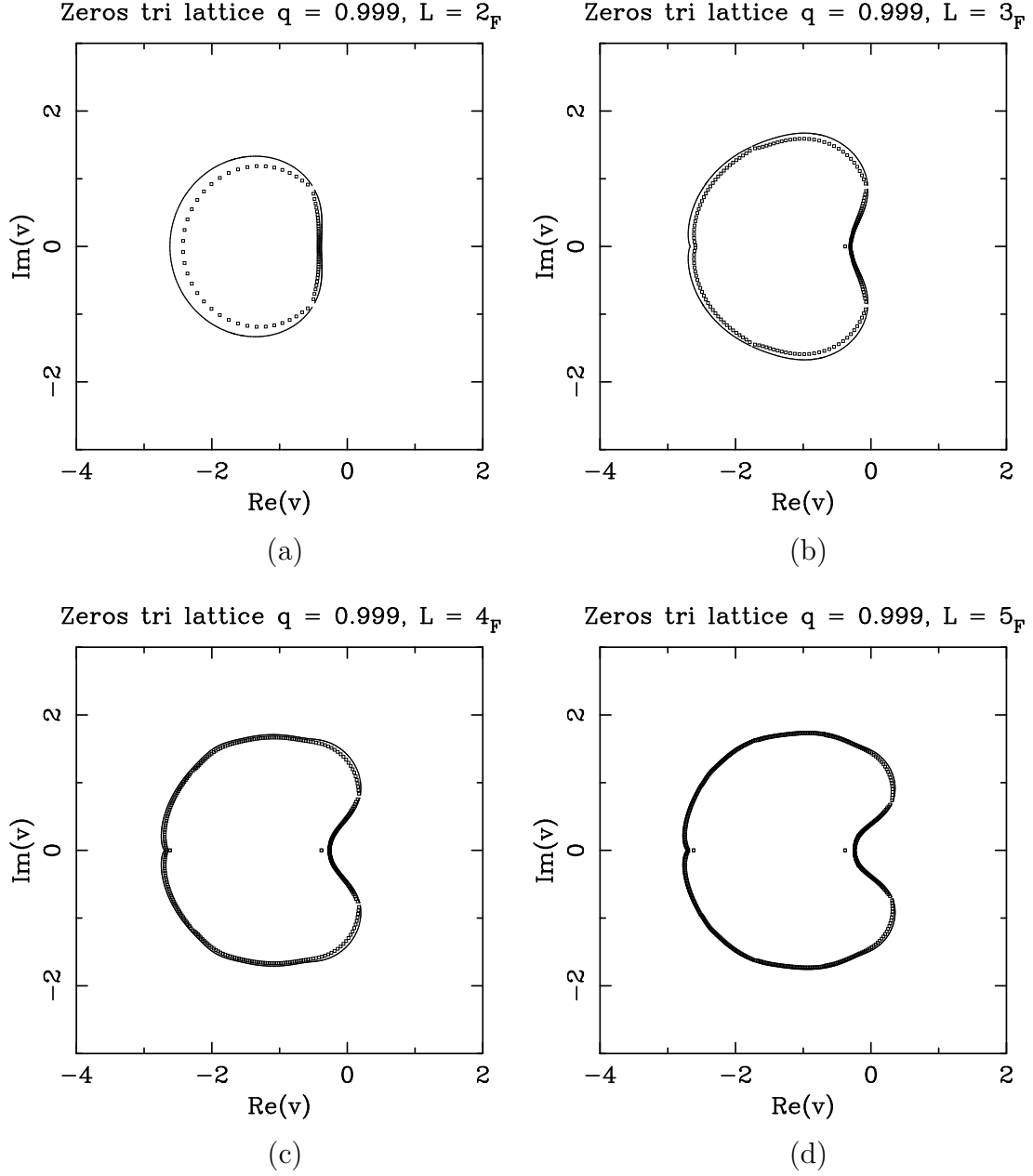
Figure 4: Limiting curves forming the singular locus $\mathcal{B}$, in the v plane, for the free energy of the Potts model for $q = 0.999$ on the $L_F \times \infty_F$ triangular-lattice strips with (a) $L = 2$, (b) $L = 3$, (c) $L = 4$, and (d) $L = 5$. This are essentially equivalent to the limiting curves for f_{qn} at $q = 1$. We also show the partition-function zeros corresponding to the strips $L_F \times (10L)_F$ for each value of L.
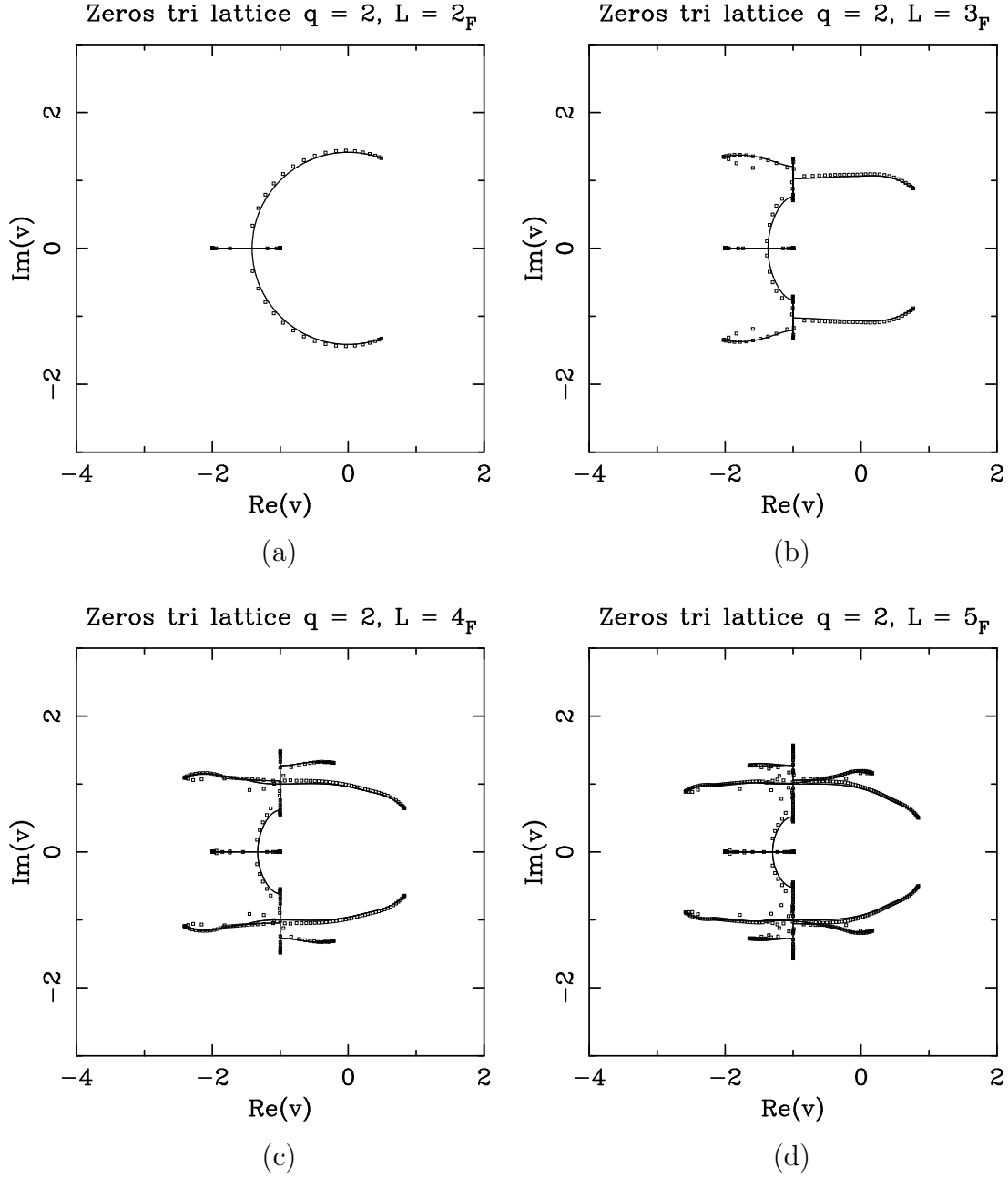
Figure 5: Limiting curves forming the singular locus $\mathcal{B}$, in the v plane, for the free energy of the Potts model for $q = 2$ on the $L_F \times \infty_F$ triangular-lattice strips with (a) $L = 2$, (b) $L = 3$, (c) $L = 4$, and (d) $L = 5$. We also show the partition-function zeros corresponding to the strips $L_F \times (10L)_F$ for each value of L. Where the results for $2 \le L \le 4$ overlap with those in [4, 5], they agree and are included here for comparison.
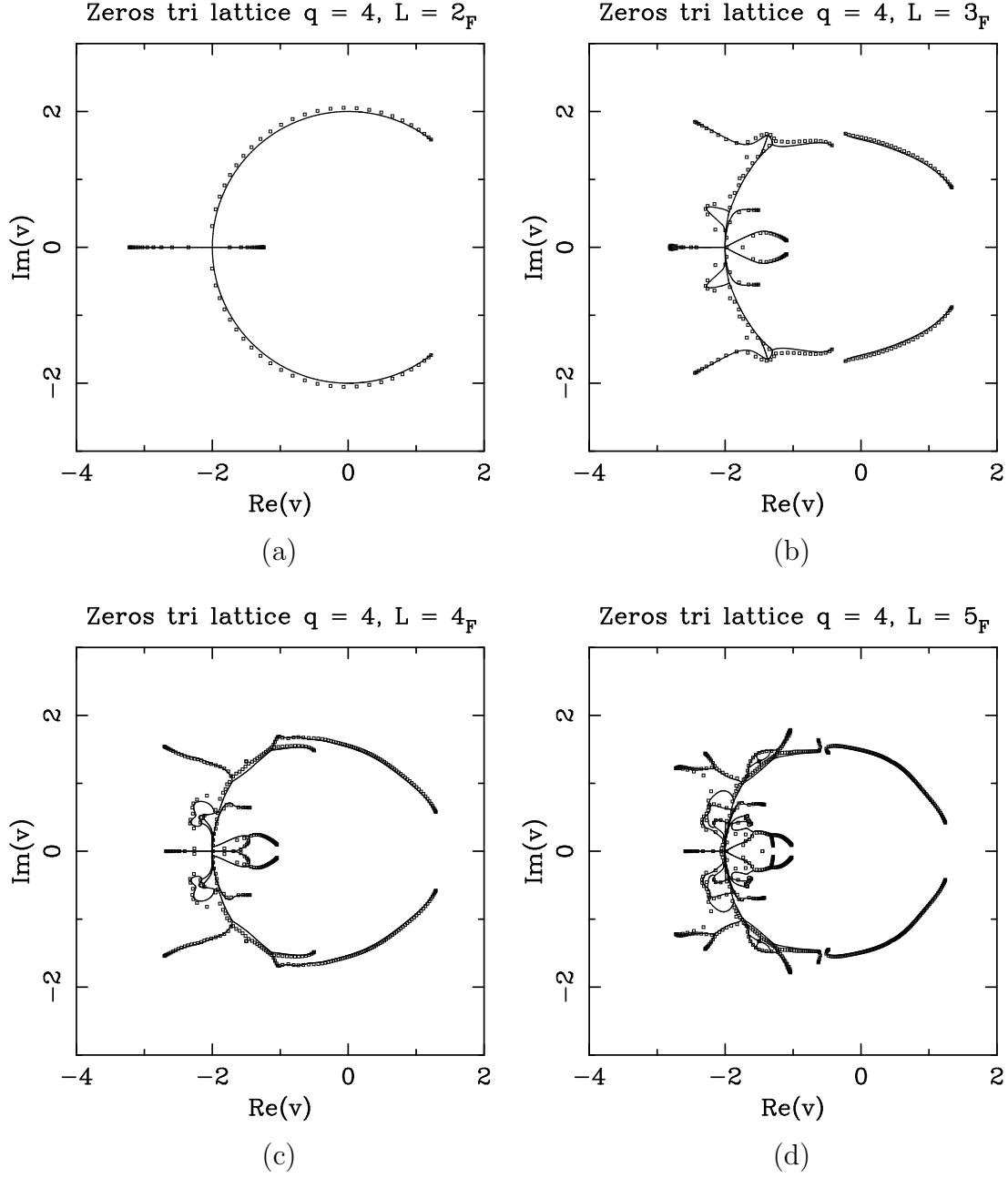
Figure 6: Limiting curves forming the singular locus $\mathcal{B}$, in the v plane, for the free energy of the Potts model for $q = 3$ on the $L_{\mathrm{F}} \times \infty_{\mathrm{F}}$ triangular-lattice strips with (a) $L = 2$, (b) $L = 3$, (c) $L = 4$, and (d) $L = 5$. We also show the partition-function zeros corresponding to the strips $L_{\mathrm{F}} \times (10L)_{\mathrm{F}}$ for each value of L. Where the results for $2 \leq L \leq 4$ overlap with those in [4, 5], they agree and are included here for comparison.

Figure 7: Limiting curves forming the singular locus $\mathcal{B}$, in the v plane, for the free energy of the Potts model for $q = 4$ on the $L_F \times \infty_F$ triangular-lattice strips with (a) $L = 2$, (b) $L = 3$, (c) $L = 4$, and (d) $L = 5$. Where the results for $2 \leq L \leq 4$ overlap with those in [4, 5], they agree and are included here for comparison. We also show the partition-function zeros corresponding to the strips $L_F \times (10L)_F$ for each value of L.
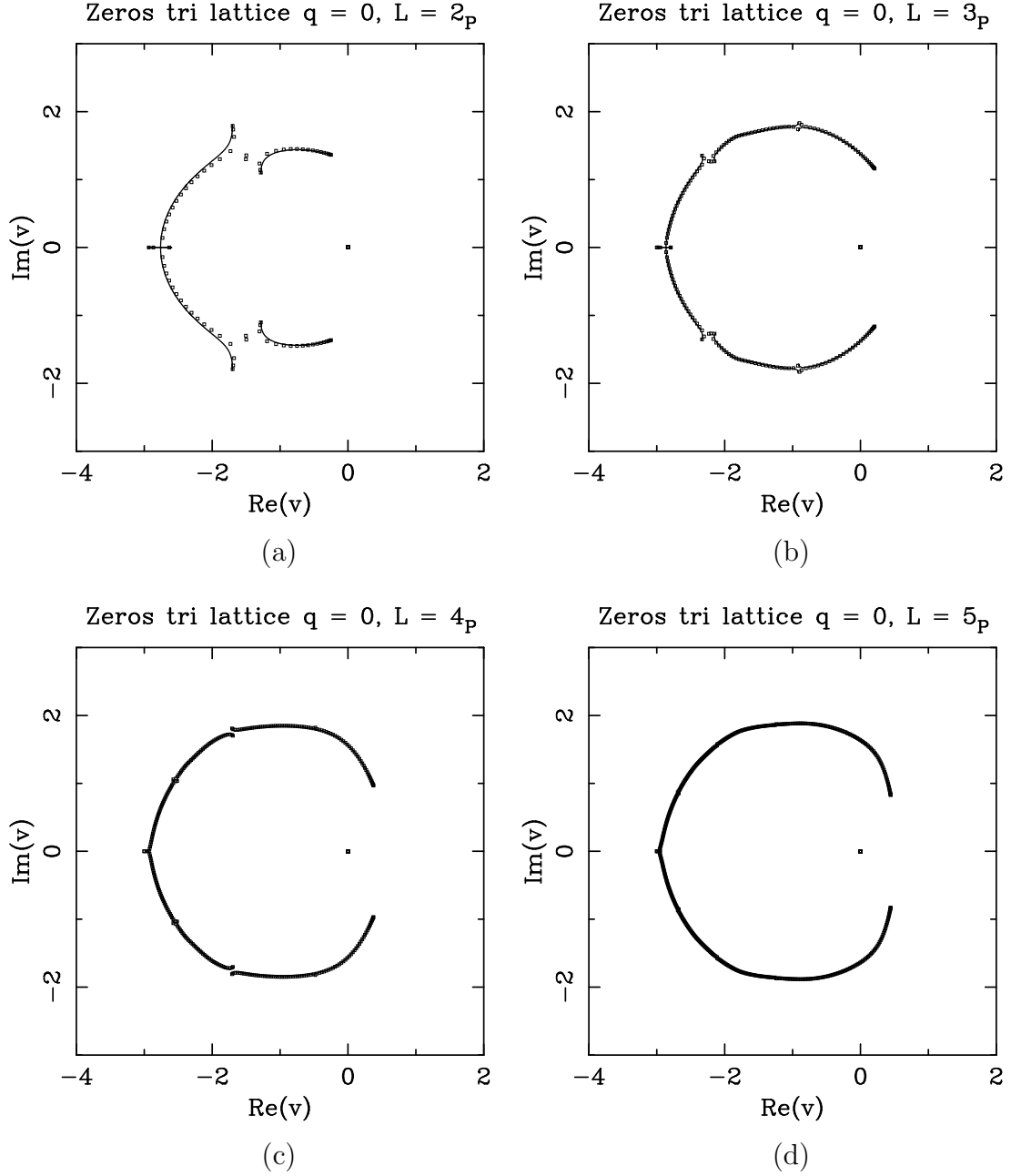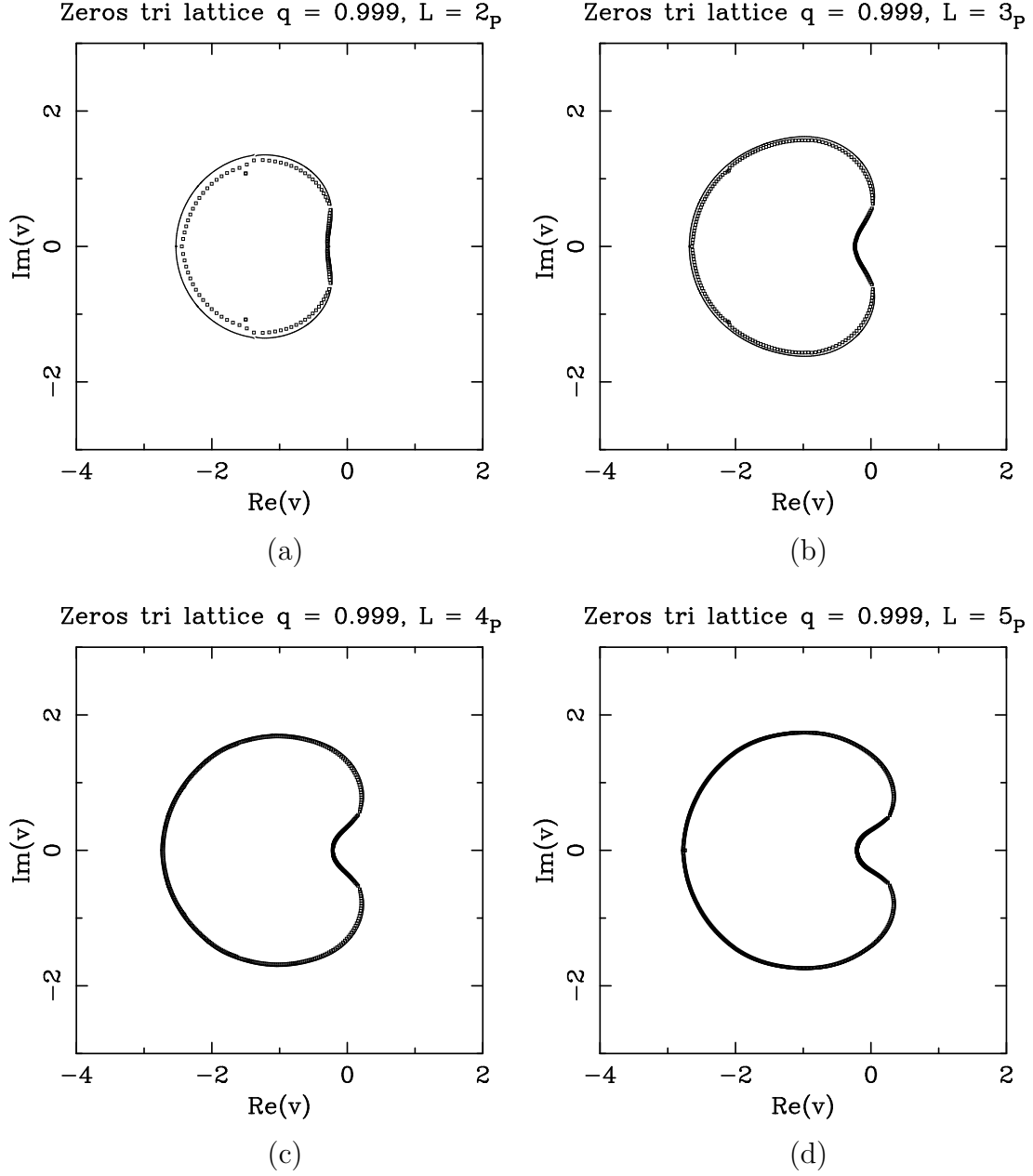
Figure 8: Limiting curves forming the singular locus $\mathcal{B}$, in the v plane, for the free energy of the Potts model, defined with the order f_{qn}, for $q = 0$ on the $L_\mathrm{P} \times \infty_\mathrm{F}$ triangular-lattice strips with (a) $L = 2$, (b) $L = 3$, (c) $L = 4$, and (d) $L = 5$. We also show the zeros of $Z(G, 0, v)/q$ corresponding to the strips $L_\mathrm{P} \times (10L)_\mathrm{F}$ for each value of L.
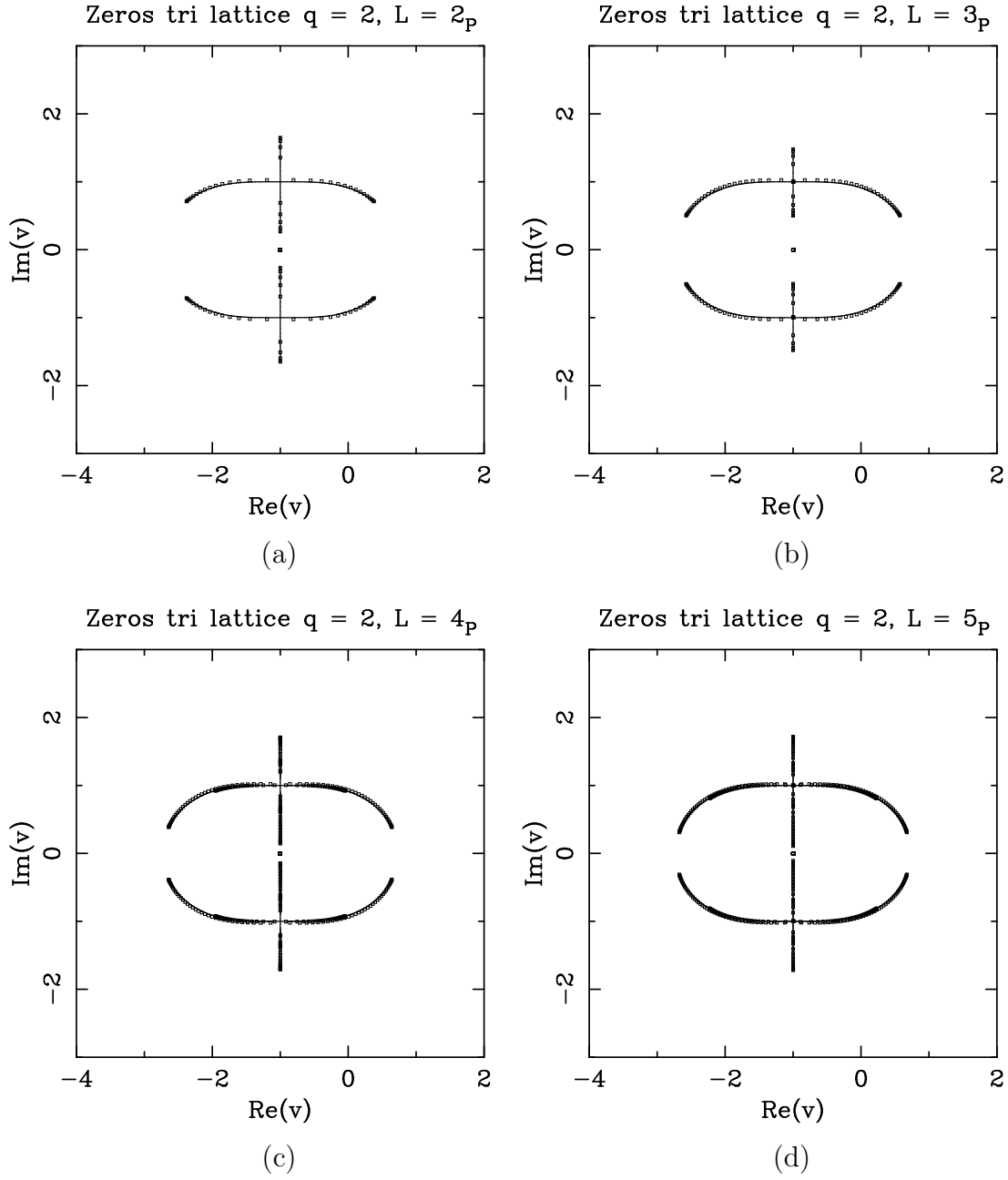
Figure 9: Limiting curves forming the singular locus $\mathcal{B}$, in the v plane, for the free energy of the Potts model for $q = 0.999$ on the $L_{\mathrm{P}} \times \infty_{\mathrm{F}}$ triangular-lattice strips with (a) $L = 2$, (b) $L = 3$, (c) $L = 4$, and (d) $L = 5$. These are essentially equivalent to the limiting curves for f_{qn} at $q = 1$. We also show the partition-function zeros corresponding to the strips $L_{\mathrm{P}} \times (10L)_{\mathrm{F}}$ for each value of L.
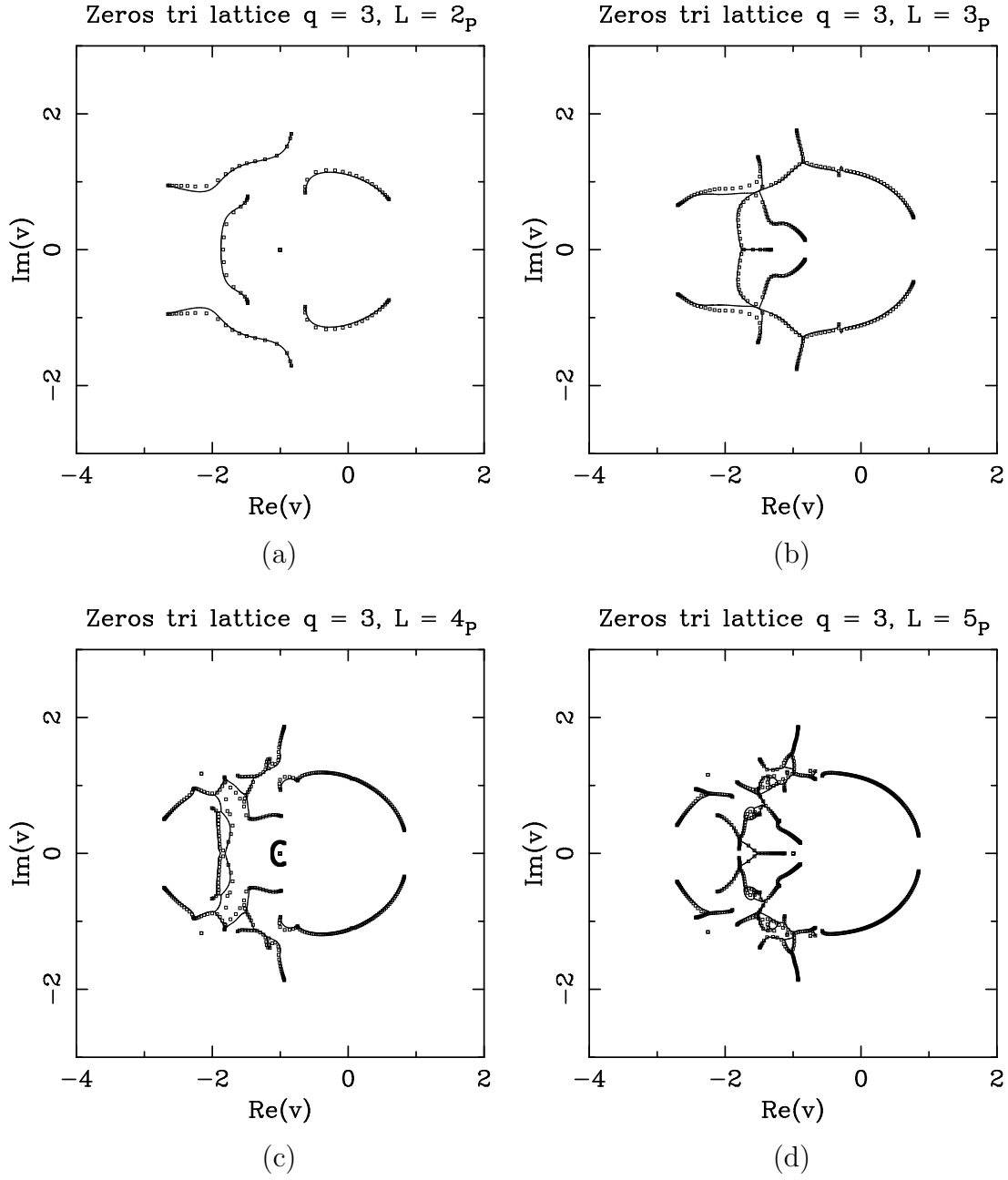
Figure 10: Limiting curves forming the singular locus $\mathcal{B}$, in the v plane, for the free energy of the Potts model for $q = 2$ on the $L_{\mathrm{P}} \times \infty_{\mathrm{F}}$ triangular-lattice strips with (a) $L = 2$, (b) $L = 3$, (c) $L = 4$, and (d) $L = 5$. We also show the partition-function zeros corresponding to the strips $L_{\mathrm{P}} \times (10L)_{\mathrm{F}}$ for each value of L.

Zeros tri lattice q = 3, L = 2$_P$

Zeros tri lattice q = 3, L = 3$_P$

(a)

(b)

Zeros tri lattice q = 3, L = 4$_P$

Zeros tri lattice q = 3, L = 5$_P$

(c)

(d)

Figure 11: Limiting curves forming the singular locus $\mathcal{B}$, in the v plane, for the free energy of the Potts model for $q = 3$ on the $L_P \times \infty_F$ triangular-lattice strips with (a) $L = 2$, (b) $L = 3$, (c) $L = 4$, and (d) $L = 5$. We also show the partition-function zeros corresponding to the strips $L_P \times (10L)_F$ for each value of L.
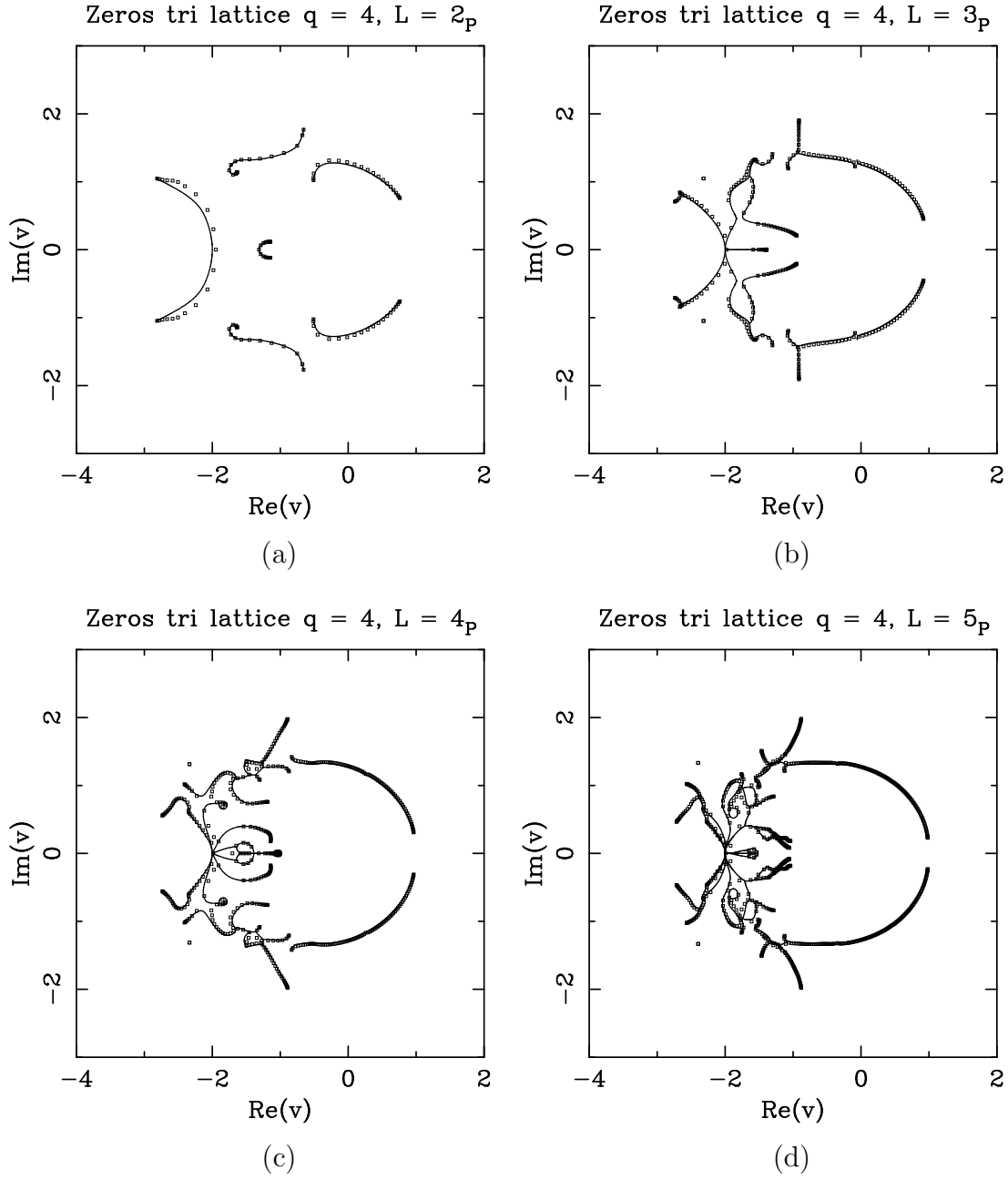
Figure 12: Limiting curves forming the singular locus $\mathcal{B}$, in the v plane, for the free energy of the Potts model for $q = 4$ on the $L_{\mathrm{P}} \times \infty_{\mathrm{F}}$ triangular-lattice strips with (a) $L = 2$, (b) $L = 3$, (c) $L = 4$, and (d) $L = 5$. We also show the partition-function zeros corresponding to the strips $L_{\mathrm{P}} \times (10L)_{\mathrm{F}}$ for each value of L.
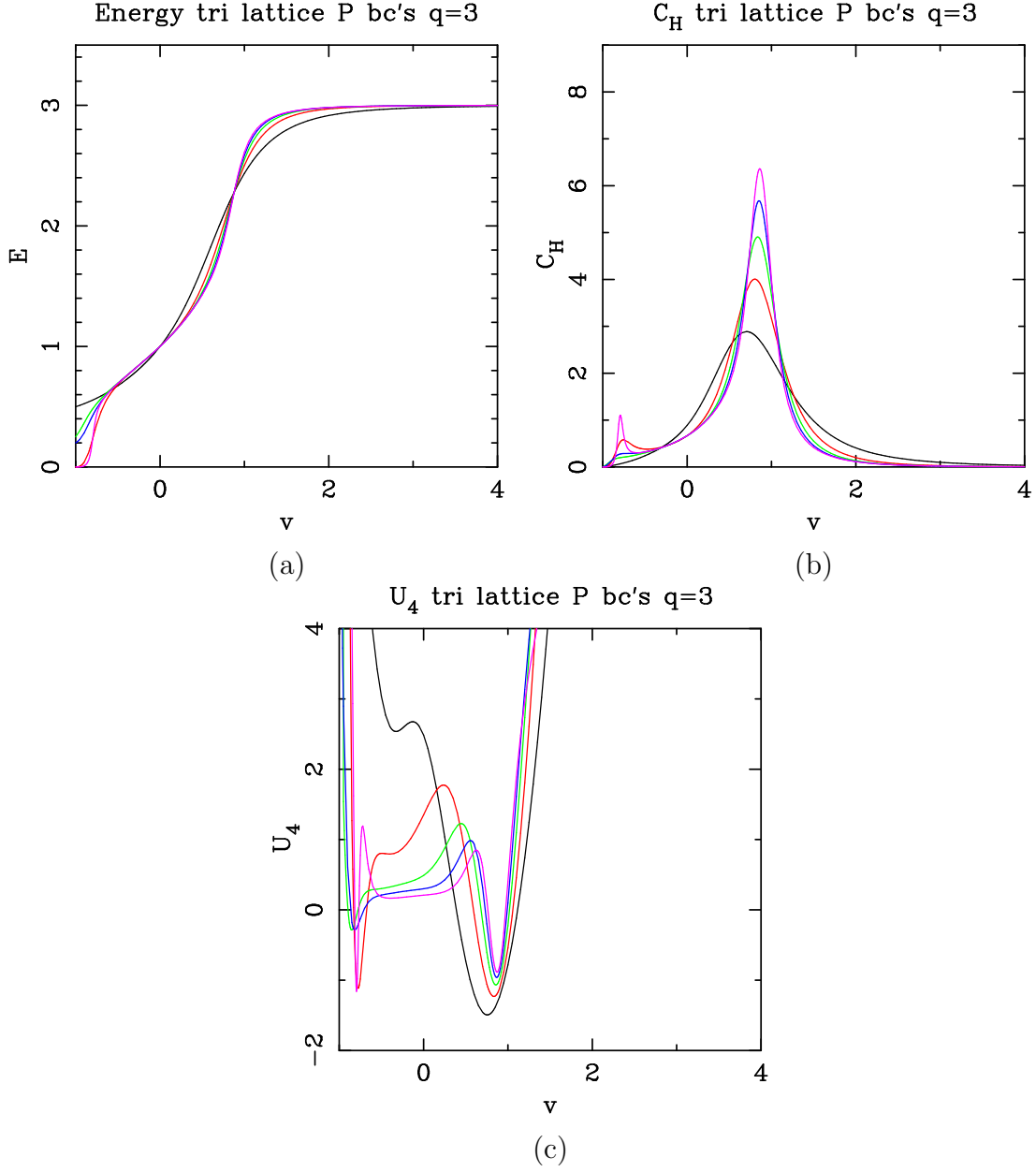
Figure 13: Thermodynamic observables for the 3-state Potts model on triangular-lattice strips of sizes $L_P \times \infty_F$. We show (a) the energy density E, (b) the specific heat C_H, and (c) the Binder cumulant U_4 as a function of the temperature-like parameter v for several strip widths L: 2 (black), 3 (red), 4 (green), 5 (blue), and 6 (pink). $-1 \leq v < 0$ corresponds to the antiferromagnetic regime, while $v > 0$ to the ferromagnetic one.